

PARTICLE PHYSICS AND COSMOLOGY

JOHN ELLIS

*Theoretical Physics Division, CERN, CH- 1211 Geneva 23, Switzerland
E-mail: John.Ellis@cern.ch*

In the first Lecture, the Big Bang and the Standard Model of particle physics are introduced, as well as the structure of the latter and open issues beyond it. Neutrino physics is discussed in the second Lecture, with emphasis on models for neutrino masses and oscillations. The third Lecture is devoted to supersymmetry, including the prospects for discovering it at accelerators or as cold dark matter. Inflation is reviewed from the viewpoint of particle physics in the fourth Lecture, including simple models with a single scalar inflaton field: the possibility that this might be a sneutrino is proposed. Finally, the fifth Lecture is devoted to topics further beyond the Standard Model, such as grand unification, baryo- and leptogenesis - that might be due to sneutrino inflaton decays - and ultra-high-energy cosmic rays - that might be due to the decays of metastable superheavy dark matter particles.

*Lectures presented at the Australian National University Summer School on the
New Cosmology, Canberra, January 2003
CERN-TH/2003-098 astro-ph/0305038*

1 Introduction to the Standard Models

1.1 The Big Bang and Particle Physics

The Universe is currently expanding almost homogeneously and isotropically, as discovered by Hubble, and the radiation it contains is cooling as it expands adiabatically:

$$a \times T \simeq \text{Constant}, \quad (1)$$

where a is the scale factor of the Universe and T is the temperature. There are two important pieces of evidence that the scale factor of the Universe was once much smaller than it is today, and correspondingly that its temperature was much higher. One is the *Cosmic Microwave Background*¹, which bathes us in photons with a density

$$n_\gamma \simeq 400 \text{ cm}^{-3}, \quad (2)$$

with an effective temperature $T \simeq 2.7$ K. These photons were released when electrons and nuclei combined to form atoms, when the Universe was some 3000 times hotter and the scale factor correspondingly 3000 times smaller than it is today. The second is the agreement of the *Abundances of Light Elements*², in particular those of ⁴He, Deuterium and ⁶Li, with calculations of cosmological nucleosynthesis. For these elements to have been produced by nuclear fusion, the Universe must once have been some 10⁹ times hotter and smaller than it is today.

During this epoch of the history of the Universe, its energy density would have been dominated by relativistic particles such as photons and neutrinos, in which

case the age t of the Universe is given approximately by

$$t \propto a^2 \propto \frac{1}{T^2}. \quad (3)$$

The constant of proportionality between time and temperature is such that $t \simeq 1$ second when the temperature $T \simeq 1$ MeV, near the start of cosmological nucleosynthesis. Since typical particle energies in a thermal plasma are $\mathcal{O}(T)$, and the Boltzmann distribution guarantees large densities of particles weighing $\mathcal{O}(T)$, the history of the earlier Universe when $T > \mathcal{O}(1)$ MeV was dominated by elementary particles weighing an MeV or more ³.

The landmarks in the history of the Universe during its first second presumably included the epoch when protons and neutrons were created out of quarks, when $T \sim 200$ MeV and $t \sim 10^{-5}$ s. Prior to that, there was an epoch when the symmetry between weak and electromagnetic interactions was broken, when $T \sim 100$ GeV and $t \sim 10^{-10}$ s. Laboratory experiments with accelerators have already explored physics at energies $E \lesssim 100$ GeV, and the energy range $E \lesssim 1000$ GeV, corresponding to the history of the Universe when $t \gtrsim 10^{-12}$ s, will be explored at CERN's LHC accelerator that is scheduled to start operation in 2007 ⁴. Our ideas about physics at earlier epochs are necessarily more speculative, but one possibility is that there was an inflationary epoch when the age of the Universe was somewhere between 10^{-40} and 10^{-30} s.

We return later to possible experimental probes of the physics of these early epochs, but first we review the Standard Model of particle physics, which underlies our description of the Universe since it was 10^{-10} s old.

1.2 Summary of the Standard Model of Particle Physics

The Standard Model of particle physics has been established by a series of experiments and theoretical developments over the past century ⁵, including:

- 1897 - The discovery of the electron;
- 1910 - The discovery of the nucleus;
- 1930 - The nucleus found to be made of protons and neutrons; neutrino postulated;
- 1936 - The muon discovered;
- 1947 - Pion and strange particles discovered;
- 1950's - Many strongly-interacting particles discovered;
- 1964 - Quarks proposed;
- 1967 - The Standard Model proposed;
- 1973 - Neutral weak interactions discovered;
- 1974 - The charm quark discovered;

- 1975 - The τ lepton discovered;
- 1977 - The bottom quark discovered;
- 1979 - The gluon discovered;
- 1983 - The intermediate W^\pm, Z^0 bosons discovered;
- 1989 - Three neutrino species counted;
- 1994 - The top quark discovered;
- 1998 - Neutrino oscillations discovered.

All the above historical steps, apart from the last (which was made with neutrinos from astrophysical sources), fit within the Standard Model, and the Standard Model continues to survive all experimental tests at accelerators.

The Standard Model contains the following set of spin-1/2 matter particles:

$$\text{Leptons : } \begin{pmatrix} \nu_e \\ e \end{pmatrix}, \begin{pmatrix} \nu_\mu \\ \mu \end{pmatrix}, \begin{pmatrix} \nu_\tau \\ \tau \end{pmatrix} \quad (4)$$

$$\text{Quarks : } \begin{pmatrix} u \\ d \end{pmatrix}, \begin{pmatrix} c \\ s \end{pmatrix}, \begin{pmatrix} b \\ t \end{pmatrix} \quad (5)$$

We know from experiments at CERN's LEP accelerator in 1989 that there can only be three neutrinos ⁶:

$$N_\nu = 2.9841 \pm 0.0083, \quad (6)$$

which is a couple of standard deviations below 3, but that cannot be considered a significant discrepancy. I had always hoped that N_ν might turn out to be non-integer: $N_\nu = \pi$ would have been good, and $N_\nu = e$ would have been even better, but this was not to be! The constraint (6) is also important for possible physics beyond the Standard Model, such as supersymmetry as we discuss later. The measurement (6) implies, by extension, that there can only be three charged leptons and hence no more quarks, by analogy and in order to preserve the calculability of the Standard Model ⁷.

The forces between these matter particles are carried by spin-1 bosons: electromagnetism by the familiar massless photon γ , the weak interactions by the massive intermediate W^\pm and Z^0 bosons that weigh $\simeq 80, 91$ GeV, respectively, and the strong interactions by the massless gluon. *Among the key objectives of particle physics are attempts to unify these different interactions, and to explain the very different masses of the various matter particles and spin-1 bosons.*

Since the Standard Model is the rock on which our quest for new physics must be built, we now review its basic features ⁵ and examine whether its successes offer any hint of the direction in which to search for new physics. Let us first recall the structure of the charged-current weak interactions, which have the current-current form:

$$\frac{1}{4} \mathcal{L}_{cc} = \frac{G_F}{\sqrt{2}} J_\mu^+ J^{-\mu}, \quad (7)$$

where the charged currents violate parity maximally:

$$J_\mu^+ = \sum_{\ell=e,\mu,\tau} \bar{\ell} \gamma_\mu (1 - \gamma_5) \nu_\ell + \text{similarly for quarks.} \quad (8)$$

The charged current (8) can be interpreted as a generator of a weak SU(2) isospin symmetry acting on the matter-particle doublets in (5). The matter fermions with left-handed helicities are doublets of this weak SU(2), whereas the right-handed matter fermions are singlets. It was suggested already in the 1930's, and with more conviction in the 1960's, that the structure (8) could most naturally be obtained by exchanging massive W^\pm vector bosons with coupling g and mass m_W :

$$\frac{G_F}{\sqrt{2}} \equiv \frac{g^2}{8m_W^2}. \quad (9)$$

In 1973, neutral weak interactions with an analogous current-current structure were discovered at CERN:

$$\frac{1}{4} \mathcal{L}_{NC} = \frac{G_F^{NC}}{\sqrt{2}} J_\mu^0 J^{\mu 0}, \quad (10)$$

and it was natural to suggest that these might also be carried by massive neutral vector bosons Z^0 .

The W^\pm and Z^0 bosons were discovered at CERN in 1983, so let us now review the theory of them, as well as the Higgs mechanism of spontaneous symmetry breaking by which we believe they acquire masses⁸. The vector bosons are described by the Lagrangian

$$\mathcal{L} = -\frac{1}{4} G_{\mu\nu}^i G^{i\mu\nu} - \frac{1}{4} F_{\mu\nu} F^{\mu\nu} \quad (11)$$

where $G_{\mu\nu}^i \equiv \partial_\mu W_\nu^i - \partial_\nu W_\mu^i + ig\epsilon_{ijk} W_\mu^j W_\nu^k$ is the field strength for the SU(2) vector boson W_μ^i , and $F_{\mu\nu} \equiv \partial_\mu W_\nu^i - \partial_\nu W_\mu^i$ is the field strength for a U(1) vector boson B_μ that is needed when we incorporate electromagnetism. The Lagrangian (11) contains bilinear terms that yield the boson propagators, and also trilinear and quartic vector-boson interactions.

The vector bosons couple to quarks and leptons via

$$\mathcal{L}_F = - \sum_f i [\bar{f}_L \gamma^\mu D_\mu f_L + \bar{f}_R \gamma^\mu D_\mu f_R] \quad (12)$$

where the D_μ are covariant derivatives:

$$D_\mu \equiv \partial_\mu - i g \sigma_i W_\mu^i - i g' Y B_\mu \quad (13)$$

The SU(2) piece appears only for the left-handed fermions f_L , whereas the U(1) vector boson B_μ couples to both left- and right-handed components, via their respective hypercharges Y .

The origin of all the masses in the Standard Model is postulated to be a weak doublet of scalar Higgs fields, whose kinetic term in the Lagrangian is

$$\mathcal{L}_\phi = -|D_\mu \phi|^2 \quad (14)$$

and which has the magic potential:

$$\mathcal{L}_V = -V(\phi) : V(\phi) = -\mu^2 \phi^\dagger \phi + \frac{\lambda}{2} (\phi^\dagger \phi)^2 \quad (15)$$

Because of the negative sign for the quadratic term in (15), the symmetric solution $\langle 0|\phi|0\rangle = 0$ is unstable, and if $\lambda > 0$ the favoured solution has a non-zero vacuum expectation value which we may write in the form:

$$\langle 0|\phi|0\rangle = \langle 0|\phi^\dagger|0\rangle = v \begin{pmatrix} 0 \\ \frac{1}{\sqrt{2}} \end{pmatrix} : v^2 = \frac{\mu^2}{2\lambda} \quad (16)$$

corresponding to spontaneous breakdown of the electroweak symmetry.

Expanding around the vacuum: $\phi = \langle 0|\phi|0\rangle + \hat{\phi}$, the kinetic term (14) for the Higgs field yields mass terms for the vector bosons:

$$\mathcal{L}_\phi \ni -\frac{g^2 v^2}{2} W_\mu^+ W^{\mu-} - g'^2 \frac{v^2}{2} B_\mu B^\mu + g g' v^2 B_\mu W^{\mu 3} - g^2 \frac{v^2}{2} W_\mu^3 W^{\mu 3} \quad (17)$$

corresponding to masses

$$m_{W^\pm} = \frac{gv}{2} \quad (18)$$

for the charged vector bosons. The neutral vector bosons (W_μ^3, B_μ) have a 2×2 mass-squared matrix:

$$\begin{pmatrix} \frac{g^2}{2} & \frac{-gg'}{2} \\ \frac{-gg'}{2} & \frac{g'^2}{2} \end{pmatrix} v^2 \quad (19)$$

This is easily diagonalized to yield the mass eigenstates:

$$Z_\mu = \frac{gW_\mu^3 - g'B_\mu}{\sqrt{g^2 + g'^2}} : m_Z = \frac{1}{2}\sqrt{g^2 + g'^2}v ; A_\mu = \frac{g'W_\mu^3 + gB_\mu}{\sqrt{g^2 + g'^2}} : m_A = 0 \quad (20)$$

that we identify with the massive Z^0 and massless γ , respectively. It is useful to introduce the electroweak mixing angle θ_W defined by

$$\sin \theta_W = \frac{g'}{\sqrt{g^2 + g'^2}} \quad (21)$$

in terms of the weak SU(2) coupling g and the weak U(1) coupling g' . Many other quantities can be expressed in terms of $\sin \theta_W$ (21): for example, $m_W^2/m_Z^2 = \cos^2 \theta_W$.

With these boson masses, one indeed obtains charged-current interactions of the current-current form (8) shown above, and the neutral currents take the form:

$$J_\mu^0 \equiv J_\mu^3 - \sin^2 \theta_W J_\mu^{em} , G_F^{NC} \equiv \frac{g^2 + g'^2}{8m_Z^2} \quad (22)$$

The ratio of neutral- and charged-current interaction strengths is often expressed as

$$\rho = \frac{G_F^{NC}}{G_F} = \frac{m_W^2}{m_Z^2 \cos^2 \theta_W} \quad (23)$$

which takes the value unity in the Standard Model, apart from quantum corrections (loop effects).

The previous field-theoretical discussion of the Higgs mechanism can be rephrased in more physical language. It is well known that a massless vector boson such as the photon γ or gluon g has just two polarization states: $\lambda = \pm 1$. However, a massive vector boson such as the ρ has three polarization states: $\lambda = 0, \pm 1$. This third polarization state is provided by a spin-0 field. In order to make $m_{W^\pm, Z^0} \neq 0$, this should have non-zero electroweak isospin $I \neq 0$, and the simplest possibility is a complex isodoublet (ϕ^+, ϕ^0) , as assumed above. This has four degrees of freedom, three of which are eaten by the W^\pm and Z^0 as their third polarization states, leaving us with one physical Higgs boson H . Once the vacuum expectation value $|\langle 0|\phi|0\rangle| = v/\sqrt{2} : v = \mu/\sqrt{2}\lambda$ is fixed, the mass of the remaining physical Higgs boson is given by

$$m_H^2 = 2\mu^2 = 4\lambda v^2, \quad (24)$$

which is a free parameter in the Standard Model.

1.3 Precision Tests of the Standard Model

The quantity that was measured most accurately at LEP was the mass of the Z^0 boson ⁶:

$$m_Z = 91,187.5 \pm 2.1 \text{ MeV}, \quad (25)$$

as seen in Fig. 1. Strikingly, m_Z is now known more accurately than the muon decay constant! Attaining this precision required understanding astrophysical effects - those of terrestrial tides on the LEP beam energy, which were $\mathcal{O}(10)$ MeV, as well as meteorological - when it rained, the water expanded the rock in which LEP was buried, again changing the beam energy, and seasonal - variations in the level of water in Lake Geneva also caused the rock around LEP to expand and contract - as well as electrical - stray currents from the nearby electric train line affected the LEP magnets ⁹.

LEP experiments also made precision measurements of many properties of the Z^0 boson ⁶, such as the total cross section:

$$\sigma = \frac{12\pi}{m_Z^2} \frac{\Gamma_{ee}\Gamma_{had}}{\Gamma_Z^2}, \quad (26)$$

where $\Gamma_Z(\Gamma_{ee}, \Gamma_{had})$ is the total Z^0 decay rate (rate for decays into e^+e^- , hadrons). Eq. (26) is the classical (tree-level) expression, which is reduced by about 30 % by radiative corrections. The total decay rate is given by:

$$\Gamma_Z = \Gamma_{ee} + \Gamma_{\mu\mu} + \Gamma_{\tau\tau} + N_\nu\Gamma_{\nu\nu} + \Gamma_{had}, \quad (27)$$

where we expect $\Gamma_{ee} = \Gamma_{\mu\mu} = \Gamma_{\tau\tau}$ because of lepton universality, which has been verified experimentally, as seen in Fig. 2 ⁶. Other partial decay rates have been measured via the branching ratios

$$R_{b,c} \equiv \frac{\Gamma_{\bar{b}b, \bar{c}c}}{\Gamma_{had}}, \quad (28)$$

as seen in Fig. 3.

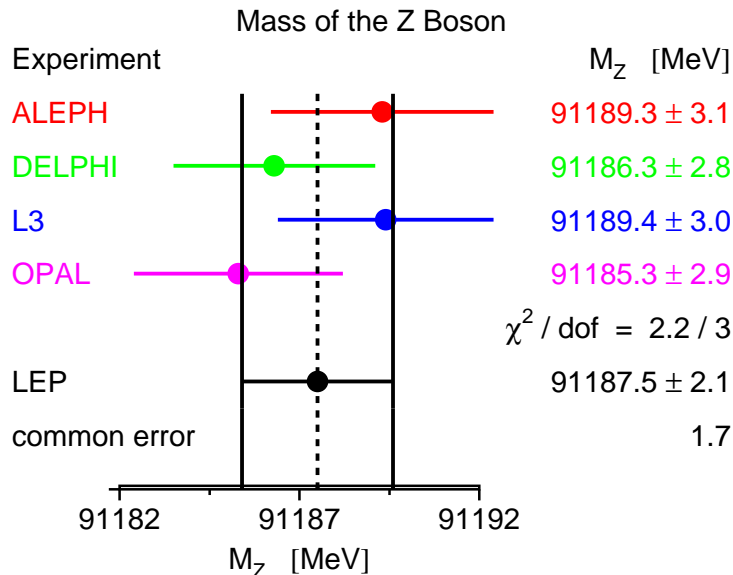


Figure 1. The mass of the Z^0 vector boson is one of the parameters of the Standard Model that has been measured most accurately ⁶.

Also measured have been various forward-backward asymmetries $A_{\ell,q}$ in the production of leptons and quarks, as well as the polarization of τ leptons produced in Z^0 decay, as also seen in Fig. 3. Various other measurements are also shown there, including the mass and decay rate of the W^\pm , the mass of the top quark, and low-energy neutral-current measurements in ν -nucleon scattering and parity violation in atomic Cesium. The Standard Model is quite compatible with all these measurements, although some of them may differ by a couple of standard deviations: if they did not, we should be suspicious! Overall, the electroweak measurements tell us that ⁶:

$$\sin^2 \theta_W = 0.23148 \pm 0.00017, \quad (29)$$

providing us with a strong hint for grand unification, as we see later.

1.4 The Search for the Higgs Boson

The precision electroweak measurements at LEP and elsewhere are sensitive to radiative corrections via quantum loop diagrams, in particular those involving particles such as the top quark and the Higgs boson that are too heavy to be observed directly at LEP ^{10,11}. Many of the electroweak observables mentioned above exhibit quadratic sensitivity to the mass of the top quark:

$$\Delta \propto G_F m_t^2. \quad (30)$$

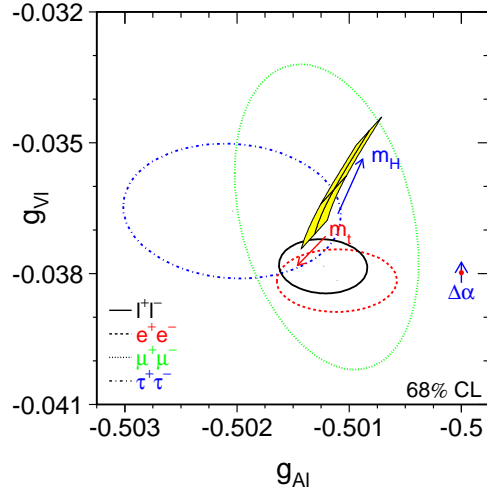


Figure 2. Precision measurements of the properties of the charged leptons e , μ and τ indicate that they have universal couplings to the weak vector bosons ⁶, whose value favours a relatively light Higgs boson.

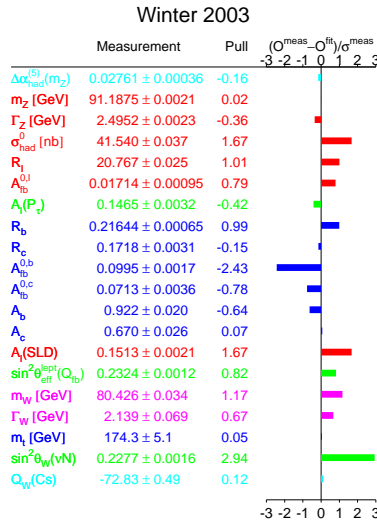


Figure 3. Precision electroweak measurements and the pulls they exert in a global fit ⁶.

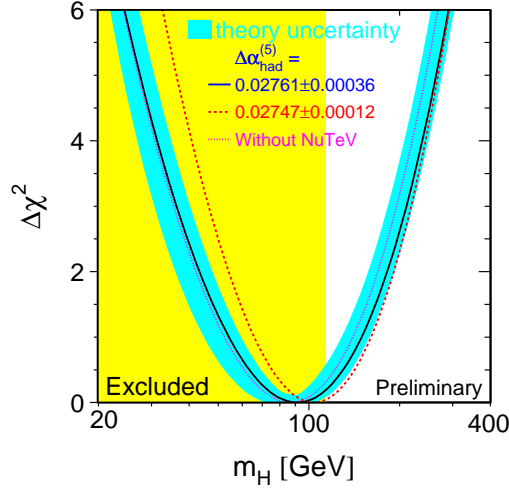


Figure 4. Estimate of the mass of the Higgs boson obtained from precision electroweak measurements. The blue band indicates theoretical uncertainties, and the different curves demonstrate the effects of different plausible estimates of the renormalization of the fine-structure constant at the Z^0 peak ⁶.

The measurements of these electroweak observables enabled the mass of the top quark to be predicted before it was discovered, and the measured value:

$$m_t = 174.3 \pm 5.1 \text{ GeV} \quad (31)$$

agrees quite well with the prediction

$$m_t = 177.5 \pm 9.3 \text{ GeV} \quad (32)$$

derived from precision electroweak data ⁶. Electroweak observables are also sensitive logarithmically to the mass of the Higgs boson:

$$\Delta \propto \left(\frac{\alpha}{\pi}\right) \ln \left(\frac{m_H^2}{m_Z^2}\right), \quad (33)$$

so their measurements can also be used to predict the mass of the Higgs boson. This prediction can be made more definite by combining the precision electroweak data with the measurement (31) of the mass of the top quark. Making due allowance for theoretical uncertainties in the Standard Model calculations, as seen in Fig. 4, one may estimate that ⁶:

$$m_H = 91_{-37}^{+58} \text{ GeV}, \quad (34)$$

whereas m_H is not known from first principles in the Standard Model.

The Higgs production and decay rates are completely fixed as functions of the unknown mass m_H , enabling the search for the Higgs boson to be planned as a

function of m_H ¹². This search was one of the main objectives of experiments at LEP, which established the lower limit:

$$m_H > 114.4 \text{ GeV}, \quad (35)$$

that is shown as the light yellow shaded region in Fig. 4. Combining this limit with the estimate (34), we see that there is good reason to expect that the Higgs boson may not be far away. Indeed, in the closing weeks of the LEP experimental programme, there was a hint for the discovery of the Higgs boson at LEP with a mass ~ 115 GeV, but this could not be confirmed ¹³. In the future, experiments at the Fermilab Tevatron collider and then the LHC will continue the search for the Higgs boson. The latter, in particular, should be able to discover it whatever its mass may be, up to the theoretical upper limit $m_H \lesssim 1 \text{ TeV}$ ⁴.

1.5 Roadmap to Physics Beyond the Standard Model

The Standard Model agrees with all confirmed experimental data from accelerators, but is theoretically very unsatisfactory ^{14,15}. It does not explain the particle quantum numbers, such as the electric charge Q , weak isospin I , hypercharge Y and colour, and contains at least 19 arbitrary parameters. These include three independent vector-boson couplings and a possible CP-violating strong-interaction parameter, six quark and three charged-lepton masses, three generalized Cabibbo weak mixing angles and the CP-violating Kobayashi-Maskawa phase, as well as two independent masses for weak bosons.

The Big Issues in physics beyond the Standard Model are conveniently grouped into three categories ^{14,15}. These include the problem of **Mass**: what is the origin of particle masses, are they due to a Higgs boson, and, if so, why are the masses so small; **Unification**: is there a simple group framework for unifying all the particle interactions, a so-called Grand Unified Theory (GUT); and **Flavour**: why are there so many different types of quarks and leptons and why do their weak interactions mix in the peculiar way observed? Solutions to all these problems should eventually be incorporated in a Theory of Everything (TOE) that also includes gravity, reconciles it with quantum mechanics, explains the origin of space-time and why it has four dimensions, makes coffee, etc. String theory, perhaps in its current incarnation of M theory, is the best (only?) candidate we have for such a TOE ¹⁶, but we do not yet understand it well enough to make clear experimental predictions.

As if the above 19 parameters were insufficient to appall you, at least nine more parameters must be introduced to accommodate the neutrino oscillations discussed in the next Lecture: 3 neutrino masses, 3 real mixing angles, and 3 CP-violating phases, of which one is in principle observable in neutrino-oscillation experiments and the other two in neutrinoless double-beta decay experiments. In fact even the simplest models for neutrino masses involve 9 further parameters, as discussed later.

Moreover, there are many other cosmological parameters that we should also seek to explain. Gravity is characterized by at least two parameters, the Newton constant G_N and the cosmological vacuum energy. We may also want to construct a field-theoretical model for inflation, and we certainly need to explain the baryon

asymmetry of the Universe. So there is plenty of scope for physics beyond the Standard Model.

The first clear evidence for physics beyond the Standard Model of particle physics has been provided by neutrino physics, which is also of great interest for cosmology, so this is the subject of Lecture 2. Since there are plenty of good reasons to study supersymmetry¹⁵, including the possibility that it provides the cold dark matter, this is the subject of Lecture 3. Inflation is the subject of Lecture 4, and various further topics such as GUTs, baryo/leptogenesis and ultra-high-energy cosmic rays are discussed in Lecture 5. As we shall see later, neutrino physics may be the key to both inflation and baryogenesis.

2 Neutrino Physics

2.1 Neutrino Masses?

There is no good reason why either the total lepton number L or the individual lepton flavours $L_{e,\mu,\tau}$ should be conserved. Theorists have learnt that the only conserved quantum numbers are those associated with exact local symmetries, just as the conservation of electromagnetic charge is associated with local U(1) invariance. On the other hand, there is no exact local symmetry associated with any of the lepton numbers, so we may expect non-zero neutrino masses.

However, so far we have only upper experimental limits on neutrino masses¹⁷. From measurements of the end-point in Tritium β decay, we know that:

$$m_{\nu_e} \lesssim 2.5 \text{ eV}, \quad (36)$$

which might be improved down to about 0.5 eV with the proposed KATRIN experiment¹⁸. From measurements of $\pi \rightarrow \mu\nu$ decay, we know that:

$$m_{\nu_\mu} < 190 \text{ KeV}, \quad (37)$$

and there are prospects to improve this limit by a factor ~ 20 . Finally, from measurements of $\tau \rightarrow n\pi\nu$ decay, we know that:

$$m_{\nu_\tau} < 18.2 \text{ MeV}, \quad (38)$$

and there are prospects to improve this limit to ~ 5 MeV.

Astrophysical upper limits on neutrino masses are stronger than these laboratory limits. The 2dF data were used to infer an upper limit on the sum of the neutrino masses of 1.8 eV¹⁹, which has recently been improved using WMAP data to²⁰

$$\Sigma_{\nu_i} m_{\nu_i} < 0.7 \text{ eV}, \quad (39)$$

as seen in Fig. 5. This impressive upper limit is substantially better than even the most stringent direct laboratory upper limit on an individual neutrino mass.

Another interesting laboratory limit on neutrino masses comes from searches for neutrinoless double- β decay, which constrain the sum of the neutrinos' Majorana masses weighted by their couplings to electrons²¹:

$$\langle m_\nu \rangle_e \equiv |\Sigma_{\nu_i} m_{\nu_i} U_{ei}^2| \lesssim 0.35 \text{ eV} \quad (40)$$

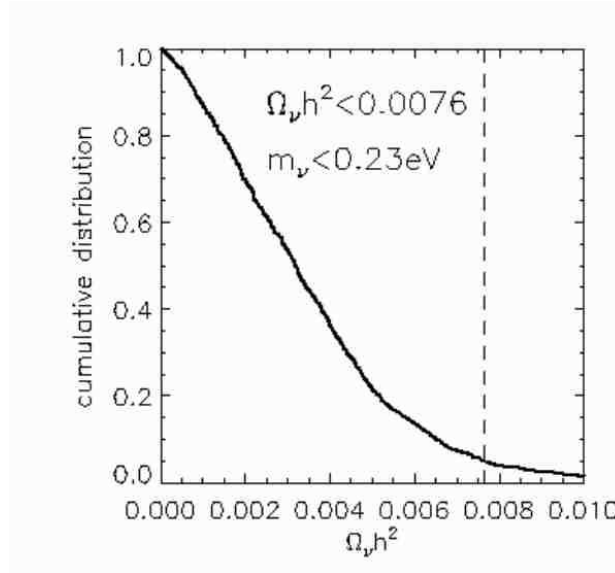


Figure 5. Likelihood function for the sum of neutrino masses provided by WMAP ²⁰: the quoted upper limit applies if the 3 light neutrino species are degenerate.

which might be improved to ~ 0.01 eV in a future round of experiments.

Neutrinos have been seen to oscillate between their different flavours ^{22,23}, showing that the separate lepton flavours $L_{e,\mu,\tau}$ are indeed not conserved, though the conservation of total lepton number L is still an open question. The observation of such oscillations strongly suggests that the neutrinos have different masses.

2.2 Models of Neutrino Masses and Mixing

The conservation of lepton number is an accidental symmetry of the renormalizable terms in the Standard Model Lagrangian. However, one could easily add to the Standard Model non-renormalizable terms that would generate neutrino masses, even without introducing any new fields. For example, a non-renormalizable term of the form ²⁴

$$\frac{1}{M}\nu H \cdot \nu H, \quad (41)$$

where M is some large mass beyond the scale of the Standard Model, would generate a neutrino mass term:

$$m_\nu \nu \cdot \nu : m_\nu = \frac{\langle 0|H|0\rangle^2}{M}. \quad (42)$$

However, a new interaction like (41) seems unlikely to be fundamental, and one should like to understand the origin of the large mass scale M .

The minimal renormalizable model of neutrino masses requires the introduction of weak-singlet ‘right-handed’ neutrinos N . These will in general couple to the

conventional weak-doublet left-handed neutrinos via Yukawa couplings Y_ν that yield Dirac masses $m_D = Y_\nu \langle 0|H|0 \rangle \sim m_W$. In addition, these ‘right-handed’ neutrinos N can couple to themselves via Majorana masses M that may be $\gg m_W$, since they do not require electroweak symmetry breaking. Combining the two types of mass term, one obtains the seesaw mass matrix ²⁵:

$$(\nu_L, N) \begin{pmatrix} 0 & M_D \\ M_D^T & M \end{pmatrix} \begin{pmatrix} \nu_L \\ N \end{pmatrix}, \quad (43)$$

where each of the entries should be understood as a matrix in generation space.

In order to provide the two measured differences in neutrino masses-squared, there must be at least two non-zero masses, and hence at least two heavy singlet neutrinos N_i ^{26,27}. Presumably, all three light neutrino masses are non-zero, in which case there must be at least three N_i . This is indeed what happens in simple GUT models such as SO(10), but some models ²⁸ have more singlet neutrinos ²⁹. In this Lecture, for simplicity we consider just three N_i .

The effective mass matrix for light neutrinos in the seesaw model may be written as:

$$\mathcal{M}_\nu = Y_\nu^T \frac{1}{M} Y_\nu v^2, \quad (44)$$

where we have used the relation $m_D = Y_\nu v$ with $v \equiv \langle 0|H|0 \rangle$. Taking $m_D \sim m_q$ or m_ℓ and requiring light neutrino masses $\sim 10^{-1}$ to 10^{-3} eV, we find that heavy singlet neutrinos weighing $\sim 10^{10}$ to 10^{15} GeV seem to be favoured.

It is convenient to work in the field basis where the charged-lepton masses $m_{\ell\pm}$ and the heavy singlet-neutrino masses M are real and diagonal. The seesaw neutrino mass matrix \mathcal{M}_ν (44) may then be diagonalized by a unitary transformation U :

$$U^T \mathcal{M}_\nu U = \mathcal{M}_\nu^d. \quad (45)$$

This diagonalization is reminiscent of that required for the quark mass matrices in the Standard Model. In that case, it is well known that one can redefine the phases of the quark fields ³⁰ so that the mixing matrix U_{CKM} has just one CP-violating phase ³¹. However, in the neutrino case, there are fewer independent field phases, and one is left with 3 physical CP-violating parameters:

$$U = \tilde{P}_2 V P_0 : P_0 \equiv \text{Diag}(e^{i\phi_1}, e^{i\phi_2}, 1). \quad (46)$$

Here $\tilde{P}_2 = \text{Diag}(e^{i\alpha_1}, e^{i\alpha_2}, e^{i\alpha_3})$ contains three phases that can be removed by phase rotations and are unobservable in light-neutrino physics, though they do play a rôle at high energies, as discussed in Lecture 5, V is the light-neutrino mixing matrix first considered by Maki, Nakagawa and Sakata (MNS) ³², and P_0 contains 2 CP-violating phases $\phi_{1,2}$ that are observable at low energies. The MNS matrix describes neutrino oscillations

$$V = \begin{pmatrix} c_{12} & s_{12} & 0 \\ -s_{12} & c_{12} & 0 \\ 0 & 0 & 1 \end{pmatrix} \begin{pmatrix} 1 & 0 & 0 \\ 0 & c_{23} & s_{23} \\ 0 & -s_{23} & c_{23} \end{pmatrix} \begin{pmatrix} c_{13} & 0 & s_{13} \\ 0 & 1 & 0 \\ -s_{13}e^{-i\delta} & 0 & c_{13}e^{-i\delta} \end{pmatrix}. \quad (47)$$

The three real mixing angles $\theta_{12,23,13}$ in (47) are analogous to the Euler angles that are familiar from the classic rotations of rigid mechanical bodies. The phase

δ is a specific quantum effect that is also observable in neutrino oscillations, and violates CP, as we discuss below. The other CP-violating phases $\phi_{1,2}$ are in principle observable in neutrinoless double- β decay (40).

2.3 Neutrino Oscillations

In quantum physics, particles such as neutrinos propagate as complex waves. Different mass eigenstates m_i travelling with the same momenta p oscillate with different frequencies:

$$e^{iE_i t} : E_i^2 = p^2 + m_i^2. \quad (48)$$

Now consider what happens if one produces a neutrino beam of one given flavour, corresponding to some specific combination of mass eigenstates. After propagating some distance, the different mass eigenstates in the beam will acquire different phase weightings (48), so that the neutrinos in the beam will be detected as a mixture of different neutrino flavours. These oscillations will be proportional to the mixing $\sin^2 2\theta$ between the different flavours, and also to the differences in masses-squared Δm_{ij}^2 between the different mass eigenstates.

The first of the mixing angles in (47) to be discovered was θ_{23} , in atmospheric neutrino experiments. Whereas the numbers of downward-going atmospheric ν_μ were found to agree with Standard Model predictions, a deficit of upward-going ν_μ was observed, as seen in Fig. 6. The data from the Super-Kamiokande experiment, in particular ²², favour near-maximal mixing of atmospheric neutrinos:

$$\theta_{23} \sim 45^\circ, \quad \Delta m_{23}^2 \sim 2.4 \times 10^{-3} \text{ eV}^2. \quad (49)$$

Recently, the K2K experiment using a beam of neutrinos produced by an accelerator has found results consistent with (49) ³³. It seems that the atmospheric ν_μ probably oscillate primarily into ν_τ , though this has yet to be established.

More recently, the oscillation interpretation of the long-standing solar-neutrino deficit has been established, in particular by the SNO experiment. Solar neutrino experiments are sensitive to the mixing angle θ_{12} in (47). The recent data from SNO ²³ and Super-Kamiokande ³⁴ prefer quite strongly the large-mixing-angle (LMA) solution to the solar neutrino problem with

$$\theta_{12} \sim 30^\circ, \quad \Delta m_{12}^2 \sim 6 \times 10^{-5} \text{ eV}^2, \quad (50)$$

though they have been unable to exclude completely the LOW solution with lower δm^2 . However, the KamLAND experiment on reactors produced by nuclear power reactors has recently found a deficit of ν_e that is highly compatible with the LMA solution to the solar neutrino problem ³⁵, as seen in Fig. 7, and excludes any other solution.

Using the range of θ_{12} allowed by the solar and KamLAND data, one can establish a correlation between the relic neutrino density $\Omega_\nu h^2$ and the neutrinoless double- β decay observable $\langle m_\nu \rangle_e$, as seen in Fig. 8 ³⁷. Pre-WMAP, the experimental limit on $\langle m_\nu \rangle_e$ could be used to set the bound

$$10^{-3} \lesssim \Omega_\nu h^2 \lesssim 10^{-1}. \quad (51)$$

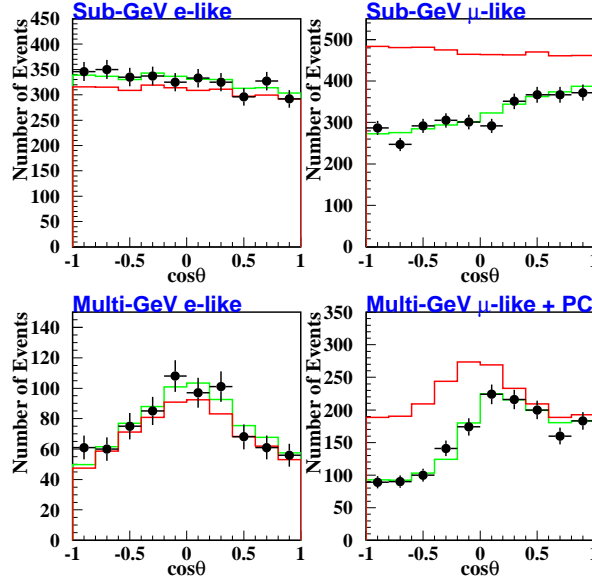


Figure 6. The zenith angle distributions of atmospheric neutrinos exhibit a deficit of downward-moving ν_μ , which is due to neutrino oscillations ²².

Alternatively, now that WMAP has set a tighter upper bound $\Omega_\nu h^2 < 0.0076$ (39) ²⁰, one can use this correlation to set an upper bound:

$$\langle m_\nu \rangle_e \lesssim 0.1 \text{ eV}, \quad (52)$$

which is difficult to reconcile with the neutrinoless double- β decay signal reported in ²¹.

The third mixing angle θ_{13} in (47) is basically unknown, with experiments such as Chooz ³⁸ and Super-Kamiokande only establishing upper limits. *A fortiori*, we have no experimental information on the CP-violating phase δ .

The phase δ could in principle be measured by comparing the oscillation probabilities for neutrinos and antineutrinos and computing the CP-violating asymmetry ³⁹:

$$P(\nu_e \rightarrow \nu_\mu) - P(\bar{\nu}_e \rightarrow \bar{\nu}_\mu) = 16s_{12}c_{12}s_{13}c_{13}^2s_{23}c_{23} \sin \delta \quad (53)$$

$$\sin\left(\frac{\Delta m_{12}^2 L}{4E}\right) \sin\left(\frac{\Delta m_{13}^2 L}{4E}\right) \sin\left(\frac{\Delta m_{23}^2 L}{4E}\right),$$

as seen in Fig. 9 ⁴⁰. This is possible only if Δm_{12}^2 and s_{12} are large enough - as now suggested by the success of the LMA solution to the solar neutrino problem, and if s_{13} is large enough - which remains an open question.

A number of long-baseline neutrino experiments using beams from accelerators are now being prepared in the United States, Europe and Japan, with the objectives of measuring more accurately the atmospheric neutrino oscillation parameters,

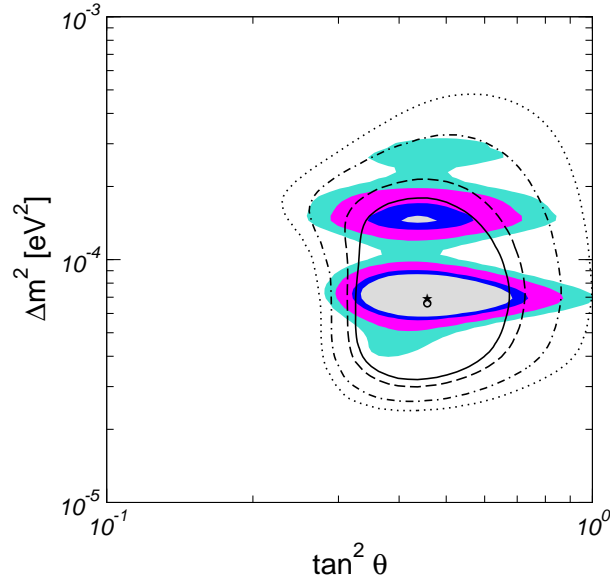


Figure 7. The KamLAND experiment (shadings) finds ³⁵ a deficit of reactor neutrinos that is consistent with the LMA neutrino oscillation parameters previously estimated (ovals) on the basis of solar neutrino experiments ³⁶.

$\Delta m_{23}^2, \theta_{23}$ and θ_{13} , and demonstrating the production of ν_τ in a ν_μ beam. Beyond these, ideas are being proposed for intense ‘super-beams’ of low-energy neutrinos, produced by high-intensity, low-energy accelerators such as the SPL ⁴¹ proposed at CERN. A subsequent step could be a storage ring for unstable ions, whose decays would produce a ‘ β beam’ of pure ν_e or $\bar{\nu}_e$ neutrinos. These experiments might be able to measure δ via CP and/or T violation in neutrino oscillations ⁴². A final step could be a full-fledged neutrino factory based on a muon storage ring, which would produce pure ν_μ and $\bar{\nu}_e$ (or ν_e and $\bar{\nu}_\mu$ beams and provide a greatly enhanced capability to search for or measure δ via CP violation in neutrino oscillations ⁴³.

We have seen above that the effective low-energy mass matrix for the light neutrinos contains 9 parameters, 3 mass eigenvalues, 3 real mixing angles and 3 CP-violating phases. However, these are not all the parameters in the minimal seesaw model. As shown in Fig. 10, this model has a total of 18 parameters ^{44,45}. The additional 9 parameters comprise the 3 masses of the heavy singlet ‘right-handed’ neutrinos M_i , 3 more real mixing angles and 3 more CP-violating phases. As illustrated in Fig. 10, many of these may be observable via renormalization in supersymmetric models ^{46,45,47,48}, which may generate observable rates for flavour-changing lepton decays such as $\mu \rightarrow e\gamma, \tau \rightarrow \mu\gamma$ and $\tau \rightarrow e\gamma$, and CP-violating observables such as electric dipole moments for the electron and muon. Some of these extra parameters may also have controlled the generation of matter in the Universe via leptogenesis ⁴⁹, as discussed in Lecture 5.

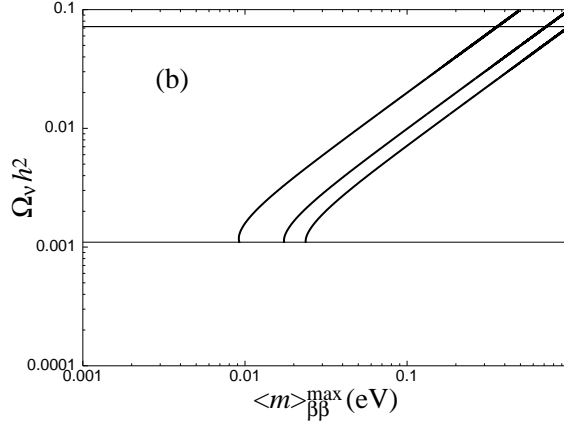


Figure 8. The correlation between the relic density of neutrinos $\Omega_\nu h^2$ and the neutrinoless double- β decay observable: the different lines indicate the ranges allowed by neutrino oscillation experiments³⁷.

3 Supersymmetry

3.1 Why?

The main theoretical reason to expect supersymmetry at an accessible energy scale is provided by the *hierarchy problem*⁵¹: why is $m_W \ll m_P$, or equivalently why is $G_F \sim 1/m_W^2 \gg G_N = 1/m_P^2$? Another equivalent question is why the Coulomb potential in an atom is so much greater than the Newton potential: $e^2 \gg G_N m^2 = m^2/m_P^2$, where m is a typical particle mass?

Your first thought might simply be to set $m_P \gg m_W$ by hand, and forget about the problem. Life is not so simple, because quantum corrections to m_H and hence m_W are quadratically divergent in the Standard Model:

$$\delta m_{H,W}^2 \simeq \mathcal{O}\left(\frac{\alpha}{\pi}\right)\Lambda^2, \quad (54)$$

which is $\gg m_W^2$ if the cutoff Λ , which represents the scale where new physics beyond the Standard Model appears, is comparable to the GUT or Planck scale. For example, if the Standard Model were to hold unscathed all the way up the Planck mass $m_P \sim 10^{19}$ GeV, the radiative correction (54) would be 36 orders of magnitude greater than the physical values of $m_{H,W}^2$!

In principle, this is not a problem from the mathematical point of view of renormalization theory. All one has to do is postulate a tree-level value of m_H^2 that is (very nearly) equal and opposite to the ‘correction’ (54), and the correct physical value may be obtained by a delicate cancellation. However, this fine tuning strikes

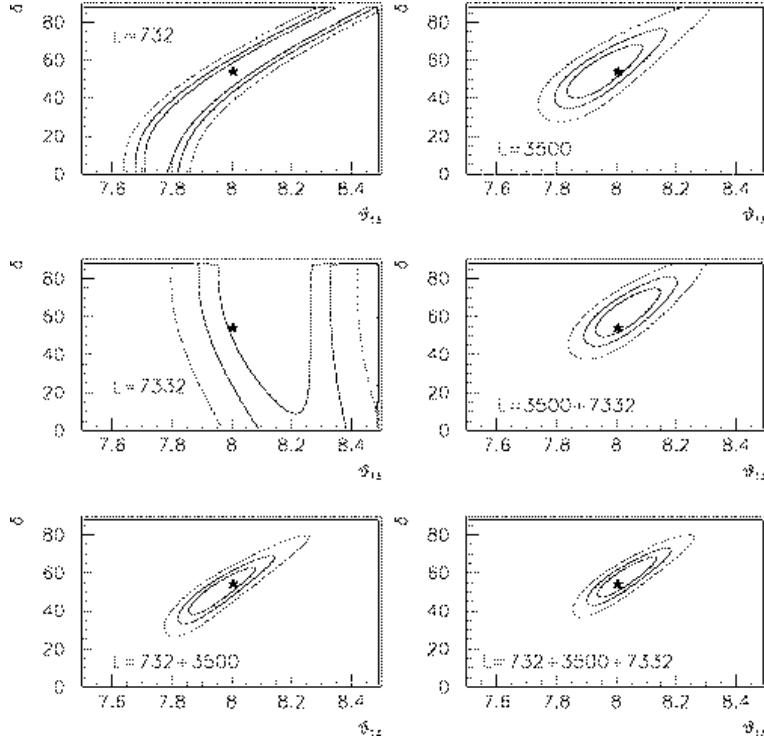


Figure 9. Possible measurements of θ_{13} and δ that could be made with a neutrino factory, using a neutrino energy threshold of about 10 GeV. Using a single baseline correlations are very strong, but can be largely reduced by combining information from different baselines and detector techniques⁴⁰, enabling the CP-violating phase δ to be extracted.

many physicists as rather unnatural: they would prefer a mechanism that keeps the ‘correction’ (54) comparable at most to the physical value⁵¹.

This is possible in a supersymmetric theory, in which there are equal numbers of bosons and fermions with identical couplings. Since bosonic and fermionic loops have opposite signs, the residual one-loop correction is of the form

$$\delta m_{H,W}^2 \simeq \mathcal{O}\left(\frac{\alpha}{\pi}\right)(m_B^2 - m_F^2), \quad (55)$$

which is $\lesssim m_{H,W}^2$ and hence naturally small if the supersymmetric partner bosons B and fermions F have similar masses:

$$|m_B^2 - m_F^2| \lesssim 1 \text{ TeV}^2. \quad (56)$$

This is the best motivation we have for finding supersymmetry at relatively low energies⁵¹. In addition to this first supersymmetric miracle of removing (55) the quadratic divergence (54), many logarithmic divergences are also absent in a supersymmetric theory⁵², a property that also plays a rôle in the construction of supersymmetric GUTs¹⁴.

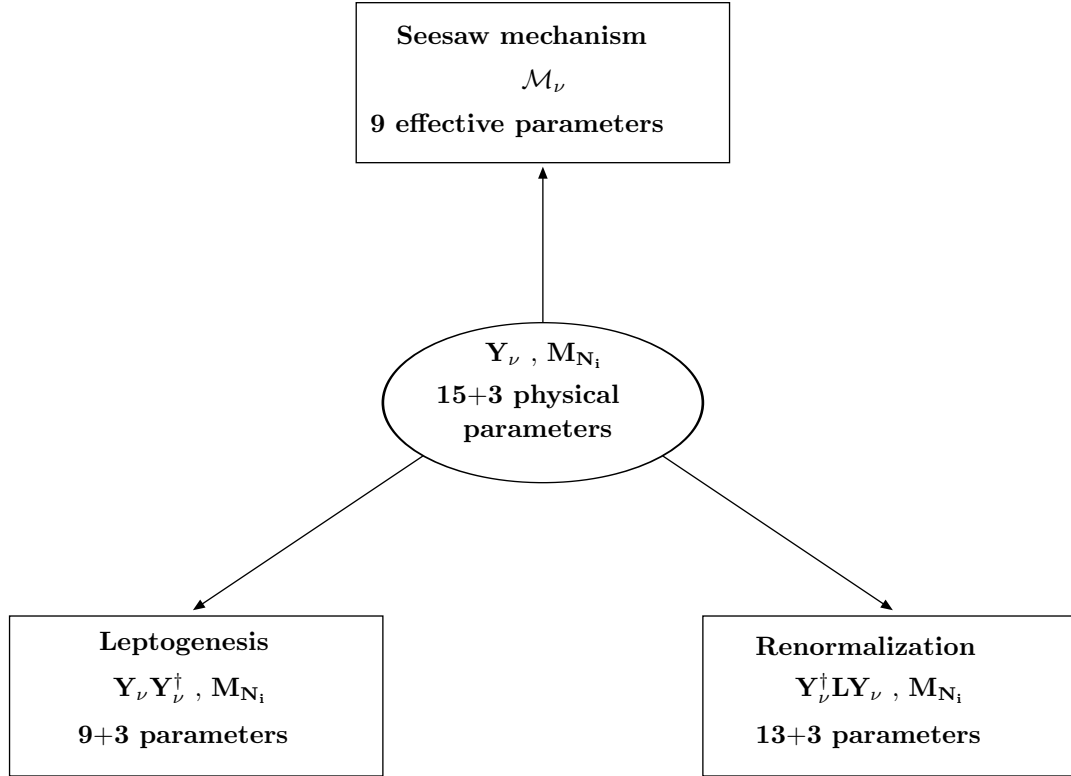


Figure 10. Roadmap for the physical observables derived from Y_ν and N_i ⁵⁰.

Supersymmetry had been around for some time before its utility for stabilizing the hierarchy of mass scales was realized. Some theorists had liked it because it offered the possibility of unifying fermionic matter particles with bosonic force-carrying particles. Some had liked it because it reduced the number of infinities found when calculating quantum corrections - indeed, theories with enough supersymmetry can even be completely finite ⁵². Theorists also liked the possibility of unifying Higgs bosons with matter particles, though the first ideas for doing this did not work out very well ⁵³. Another aspect of supersymmetry, that made some theorists think that its appearance should be inevitable, was that it was the last possible symmetry of field theory not yet known to be exploited by Nature ⁵⁴. Yet another asset was the observation that making supersymmetry a local symmetry, like the Standard Model, necessarily introduced gravity, offering the prospect of unifying *all* the particle interactions. Moreover, supersymmetry seems to be an essential requirement for the consistency of string theory, which is the best candidate we have for a Theory of Everything, including gravity. However, none of these ‘beautiful’ arguments gave a clue about the scale of supersymmetric particle masses: this was first provided by the hierarchy argument outlined above.

Could any of the known particles in the Standard Model be paired up in supermultiplets? Unfortunately, none of the known fermions q, ℓ can be paired with any of the ‘known’ bosons γ, W^\pm, Z^0, g, H , because their internal quantum numbers do not match⁵³. For example, quarks q sit in triplet representations of colour, whereas the known bosons are either singlets or octets of colour. Then again, leptons ℓ have non-zero lepton number $L = 1$, whereas the known bosons have $L = 0$. Thus, the only possibility seems to be to introduce new supersymmetric partners (spartners) for all the known particles, as seen in the Table below: quark \rightarrow squark, lepton \rightarrow slepton, photon \rightarrow photino, $Z \rightarrow$ Zino, $W \rightarrow$ Wino, gluon \rightarrow gluino, Higgs \rightarrow Higgsino. The best that one can say for supersymmetry is that it economizes on principle, not on particles!

Particle	Spin	Spartner	Spin
quark: q	$\frac{1}{2}$	squark: \tilde{q}	0
lepton: ℓ	$\frac{1}{2}$	slepton: $\tilde{\ell}$	0
photon: γ	1	photino: $\tilde{\gamma}$	$\frac{1}{2}$
W	1	wino: \tilde{W}	$\frac{1}{2}$
Z	1	zino: \tilde{Z}	$\frac{1}{2}$
Higgs: H	0	higgsino: \tilde{H}	$\frac{1}{2}$

The minimal supersymmetric extension of the Standard Model (MSSM)⁵⁵ has the same vector interactions as the Standard Model, and the particle masses arise in much the same way. However, in addition to the Standard Model particles and their supersymmetric partners in the Table, the minimal supersymmetric extension of the Standard Model (MSSM), requires two Higgs doublets H, \bar{H} with opposite hypercharges in order to give masses to all the matter fermions, whereas one Higgs doublet would have sufficed in the Standard Model. The two Higgs doublets couple via an extra coupling called μ , and it should also be noted that the ratio of Higgs vacuum expectation values

$$\tan \beta \equiv \frac{\langle \bar{H} \rangle}{\langle H \rangle} \tag{57}$$

is undetermined and should be treated as a free parameter.

3.2 Hints of Supersymmetry

There are some phenomenological hints that supersymmetry may, indeed, appear at the TeV scale. One is provided by the strengths of the different Standard Model in-

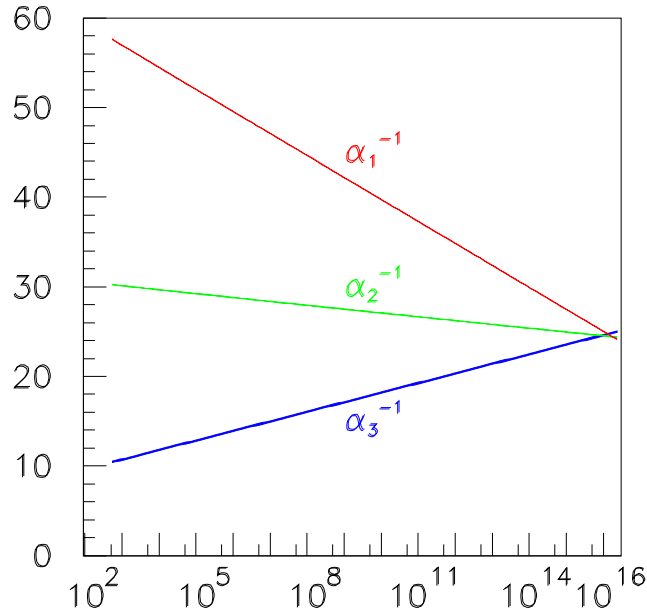


Figure 11. The measurements of the gauge coupling strengths at LEP, including $\sin^2 \theta_W$ (29), evolve to a unified value if supersymmetry is included ⁵⁶.

teractions, as measured at LEP ⁵⁶. These may be extrapolated to high energy scales including calculable renormalization effects ⁵⁷, to see whether they unify as predicted in a GUT. The answer is no, if supersymmetry is not included in the calculations. In that case, GUTs would require a ratio of the electromagnetic and weak coupling strengths, parametrized by $\sin^2 \theta_W$, different from what is observed (29), if they are to unify with the strong interactions. On the other hand, as seen in Fig. 11, minimal supersymmetric GUTs predict just the correct ratio for the weak and electromagnetic interaction strengths, i.e., value for $\sin^2 \theta_W$ (29).

A second hint is the fact that precision electroweak data prefer a relatively light Higgs boson weighing less than about 200 GeV ⁶. This is perfectly consistent with calculations in the minimal supersymmetric extension of the Standard Model (MSSM), in which the lightest Higgs boson weighs less than about 130 GeV ⁵⁸.

A third hint is provided by the astrophysical necessity of cold dark matter. This could be provided by a neutral, weakly-interacting particle weighing less than about 1 TeV, such as the lightest supersymmetric particle (LSP) χ ⁵⁹. This is expected to be stable in the MSSM, and hence should be present in the Universe today as a

cosmological relic from the Big Bang^{60,59}. Its stability arises because there is a multiplicatively-conserved quantum number called R parity, that takes the values $+1$ for all conventional particles and -1 for all sparticles⁵³. The conservation of R parity can be related to that of baryon number B and lepton number L , since

$$R = (-1)^{3B+L+2S} \quad (58)$$

where S is the spin. There are three important consequences of R conservation:

1. sparticles are always produced in pairs, e.g., $\bar{p}p \rightarrow \tilde{q}\tilde{g}X$, $e^+e^- \rightarrow \tilde{\mu} + \tilde{\mu}^-$,
2. heavier sparticles decay to lighter ones, e.g., $\tilde{q} \rightarrow q\tilde{g}$, $\tilde{\mu} \rightarrow \mu\tilde{\gamma}$, and
3. the lightest sparticle (LSP) is stable, because it has no legal decay mode.

This last feature constrains strongly the possible nature of the lightest supersymmetric sparticle⁵⁹. If it had either electric charge or strong interactions, it would surely have dissipated its energy and condensed into galactic disks along with conventional matter. There it would surely have bound electromagnetically or via the strong interactions to conventional nuclei, forming anomalous heavy isotopes that should have been detected.

A priori, the LSP might have been a sneutrino partner of one of the 3 light neutrinos, but this possibility has been excluded by a combination of the LEP neutrino counting and direct searches for cold dark matter. Thus, the LSP is often thought to be the lightest neutralino χ of spin $1/2$, which naturally has a relic density of interest to astrophysicists and cosmologists: $\Omega_\chi h^2 = \mathcal{O}(0.1)$ ⁵⁹.

Finally, a fourth hint may be coming from the measured value of the muon's anomalous magnetic moment, $g_\mu - 2$, which seems to differ slightly from the Standard Model prediction^{61,62}. If there is indeed a significant discrepancy, this would require new physics at the TeV scale or below, which could easily be provided by supersymmetry, as we see later.

3.3 Constraints on Supersymmetric Models

Important experimental constraints on supersymmetric models have been provided by the unsuccessful direct searches at LEP and the Tevatron collider. When compiling these, the supersymmetry-breaking masses of the different unseen scalar particles are often assumed to have a universal value m_0 at some GUT input scale, and likewise the fermionic partners of the vector bosons are also commonly assumed to have universal fermionic masses $m_{1/2}$ at the GUT scale - the so-called constrained MSSM or CMSSM.

The allowed domains in some of the $(m_{1/2}, m_0)$ planes for different values of $\tan\beta$ and the sign of μ are shown in Fig. 12. The various panels of this figure feature the limit $m_{\chi^\pm} \gtrsim 104$ GeV provided by chargino searches at LEP⁶³. The LEP neutrino counting and other measurements have also constrained the possibilities for light neutralinos, and LEP has also provided lower limits on slepton masses, of which the strongest is $m_{\tilde{e}} \gtrsim 99$ GeV⁶⁴, as illustrated in panel (a) of Fig. 12. The most important constraints on the supersymmetric partners of the u, d, s, c, b

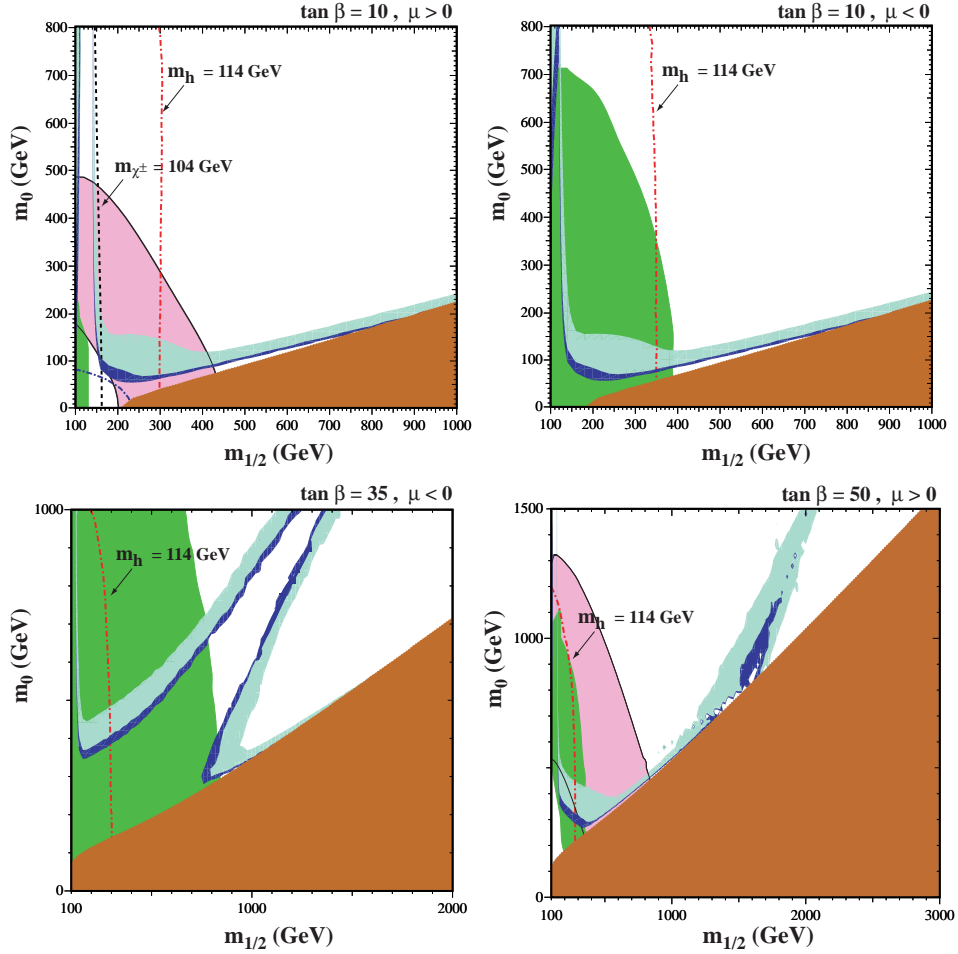


Figure 12. Compilations of phenomenological constraints on the CMSSM for (a) $\tan \beta = 10, \mu > 0$, (b) $\tan \beta = 10, \mu < 0$, (c) $\tan \beta = 35, \mu < 0$ and (d) $\tan \beta = 50, \mu > 0$ ⁶⁵. The near-vertical lines are the LEP limits $m_{\chi^\pm} = 104$ GeV (dashed and black) ⁶³, shown in (a) only, and $m_h = 114$ GeV (dotted and red) ¹³. Also, in the lower left corner of (a), we show the $m_{\tilde{e}} = 99$ GeV contour ⁶⁴. The dark (brick red) shaded regions are excluded because the LSP is charged. The light (turquoise) shaded areas have $0.1 \leq \Omega_\chi h^2 \leq 0.3$, and the smaller dark (blue) shaded regions have $0.094 \leq \Omega_\chi h^2 \leq 0.129$, as favoured by WMAP ⁶⁵. The medium (dark green) shaded regions that are most prominent in panels (b) and (c) are excluded by $b \rightarrow s\gamma$ ⁶⁶. The shaded (pink) regions in panels (a) and (d) show the $\pm 2\sigma$ ranges of $g_\mu - 2$ ⁶¹.

squarks and on the gluinos are provided by the FNAL Tevatron collider: for equal masses $m_{\tilde{q}} = m_{\tilde{g}} \gtrsim 300$ GeV. In the case of the \tilde{t} , LEP provides the most stringent limit when $m_{\tilde{t}} - m_\chi$ is small, and the Tevatron for larger $m_{\tilde{t}} - m_\chi$ ⁶³.

Another important constraint in Fig. 12 is provided by the LEP lower limit on the Higgs mass: $m_H > 114.4$ GeV ¹³. Since m_h is sensitive to sparticle masses,

particularly $m_{\tilde{t}}$, via loop corrections:

$$\delta m_h^2 \propto \frac{m_{\tilde{t}}^4}{m_W^2} \ln \left(\frac{m_{\tilde{t}}^2}{m_t^2} \right) + \dots \quad (59)$$

the Higgs limit also imposes important constraints on the soft supersymmetry-breaking CMSSM parameters, principally $m_{1/2}$ ⁶⁷ as displayed in Fig. 12.

Also shown in Fig. 12 is the constraint imposed by measurements of $b \rightarrow s\gamma$ ⁶⁶. These agree with the Standard Model, and therefore provide bounds on supersymmetric particles, such as the chargino and charged Higgs masses, in particular.

The final experimental constraint we consider is that due to the measurement of the anomalous magnetic moment of the muon. Following its first result last year ⁶⁸, the BNL E821 experiment has recently reported a new measurement ⁶¹ of $a_\mu \equiv \frac{1}{2}(g_\mu - 2)$, which deviates by about 2 standard deviations from the best available Standard Model predictions based on low-energy $e^+e^- \rightarrow$ hadrons data ⁶². On the other hand, the discrepancy is more like 0.9 standard deviations if one uses $\tau \rightarrow$ hadrons data to calculate the Standard Model prediction. Faced with this confusion, and remembering the chequered history of previous theoretical calculations ⁶⁹, it is reasonable to defer judgement whether there is a significant discrepancy with the Standard Model. However, either way, the measurement of a_μ is a significant constraint on the CMSSM, favouring $\mu > 0$ in general, and a specific region of the $(m_{1/2}, m_0)$ plane if one accepts the theoretical prediction based on $e^+e^- \rightarrow$ hadrons data ⁷⁰. The regions preferred by the current $g - 2$ experimental data and the $e^+e^- \rightarrow$ hadrons data are shown in Fig. 12.

Fig. 12 also displays the regions where the supersymmetric relic density $\rho_\chi = \Omega_\chi \rho_{critical}$ falls within the range preferred by WMAP ²⁰:

$$0.094 < \Omega_\chi h^2 < 0.129 \quad (60)$$

at the 2- σ level. The upper limit on the relic density is rigorous, but the lower limit in (60) is optional, since there could be other important contributions to the overall matter density. Smaller values of $\Omega_\chi h^2$ correspond to smaller values of $(m_{1/2}, m_0)$, in general.

We see in Fig. 12 that there are significant regions of the CMSSM parameter space where the relic density falls within the preferred range (60). What goes into the calculation of the relic density? It is controlled by the annihilation cross section ⁵⁹:

$$\rho_\chi = m_\chi n_\chi, \quad n_\chi \sim \frac{1}{\sigma_{ann}(\chi\chi \rightarrow \dots)}, \quad (61)$$

where the typical annihilation cross section $\sigma_{ann} \sim 1/m_\chi^2$. For this reason, the relic density typically increases with the relic mass, and this combined with the upper bound in (60) then leads to the common expectation that $m_\chi \lesssim \mathcal{O}(1)$ GeV.

However, there are various ways in which the generic upper bound on m_χ can be increased along filaments in the $(m_{1/2}, m_0)$ plane. For example, if the next-to-lightest sparticle (NLSP) is not much heavier than χ : $\Delta m/m_\chi \lesssim 0.1$, the relic density may be suppressed by coannihilation: $\sigma(\chi + \text{NLSP} \rightarrow \dots)$ ⁷¹. In this way,

the allowed CMSSM region may acquire a ‘tail’ extending to larger sparticle masses. An example of this possibility is the case where the NLSP is the lighter stau: $\tilde{\tau}_1$ and $m_{\tilde{\tau}_1} \sim m_\chi$, as seen in Figs. 12(a) and (b) ⁷².

Another mechanism for extending the allowed CMSSM region to large m_χ is rapid annihilation via a direct-channel pole when $m_\chi \sim \frac{1}{2}m_{Higgs}$ ^{73,74}. This may yield a ‘funnel’ extending to large $m_{1/2}$ and m_0 at large $\tan\beta$, as seen in panels (c) and (d) of Fig. 12 ⁷⁴. Yet another allowed region at large $m_{1/2}$ and m_0 is the ‘focus-point’ region ⁷⁵, which is adjacent to the boundary of the region where electroweak symmetry breaking is possible. The lightest supersymmetric particle is relatively light in this region.

3.4 Benchmark Supersymmetric Scenarios

As seen in Fig. 12, all the experimental, cosmological and theoretical constraints on the MSSM are mutually compatible. As an aid to understanding better the physics capabilities of the LHC and various other accelerators, as well as non-accelerator experiments, a set of benchmark supersymmetric scenarios have been proposed ⁷⁶. Their distribution in the $(m_{1/2}, m_0)$ plane is sketched in Fig. 13. These benchmark scenarios are compatible with all the accelerator constraints mentioned above, including the LEP searches and $b \rightarrow s\gamma$, and yield relic densities of LSPs in the range suggested by cosmology and astrophysics. The benchmarks are not intended to sample ‘fairly’ the allowed parameter space, but rather to illustrate the range of possibilities currently allowed.

In addition to a number of benchmark points falling in the ‘bulk’ region of parameter space at relatively low values of the supersymmetric particle masses, as see in Fig. 13, we also proposed ⁷⁶ some points out along the ‘tails’ of parameter space extending out to larger masses. These clearly require some degree of fine-tuning to obtain the required relic density ⁷⁷ and/or the correct W^\pm mass ⁷⁸, and some are also disfavoured by the supersymmetric interpretation of the $g_\mu - 2$ anomaly, but all are logically consistent possibilities.

3.5 Prospects for Discovering Supersymmetry at Accelerators

In the CMSSM discussed here, there are just a few prospects for discovering supersymmetry at the FNAL *Tevatron collider* ⁷⁶, but these could be increased in other supersymmetric models ⁷⁹. On the other hand, there are good prospects for discovering supersymmetry at the *LHC*, and Fig. 14 shows its physics reach for observing pairs of supersymmetric particles. The signature for supersymmetry - multiple jets (and/or leptons) with a large amount of missing energy - is quite distinctive, as seen in Fig. 15 ^{80,81}. Therefore, the detection of the supersymmetric partners of quarks and gluons at the LHC is expected to be quite easy if they weigh less than about 2.5 TeV ⁸². Moreover, in many scenarios one should be able to observe their cascade decays into lighter supersymmetric particles. As seen in Fig. 16, large fractions of the supersymmetric spectrum should be seen in most of the benchmark scenarios, although there are a couple where only the lightest

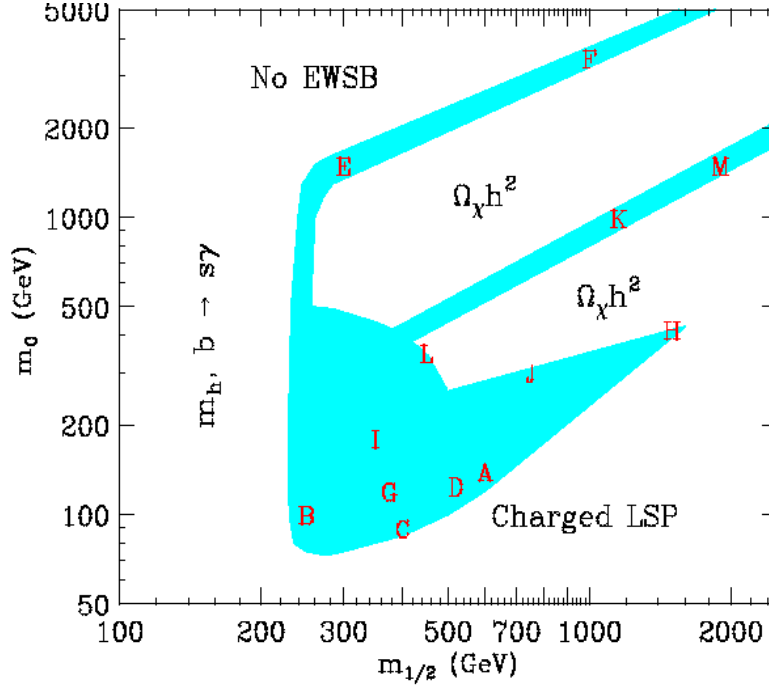
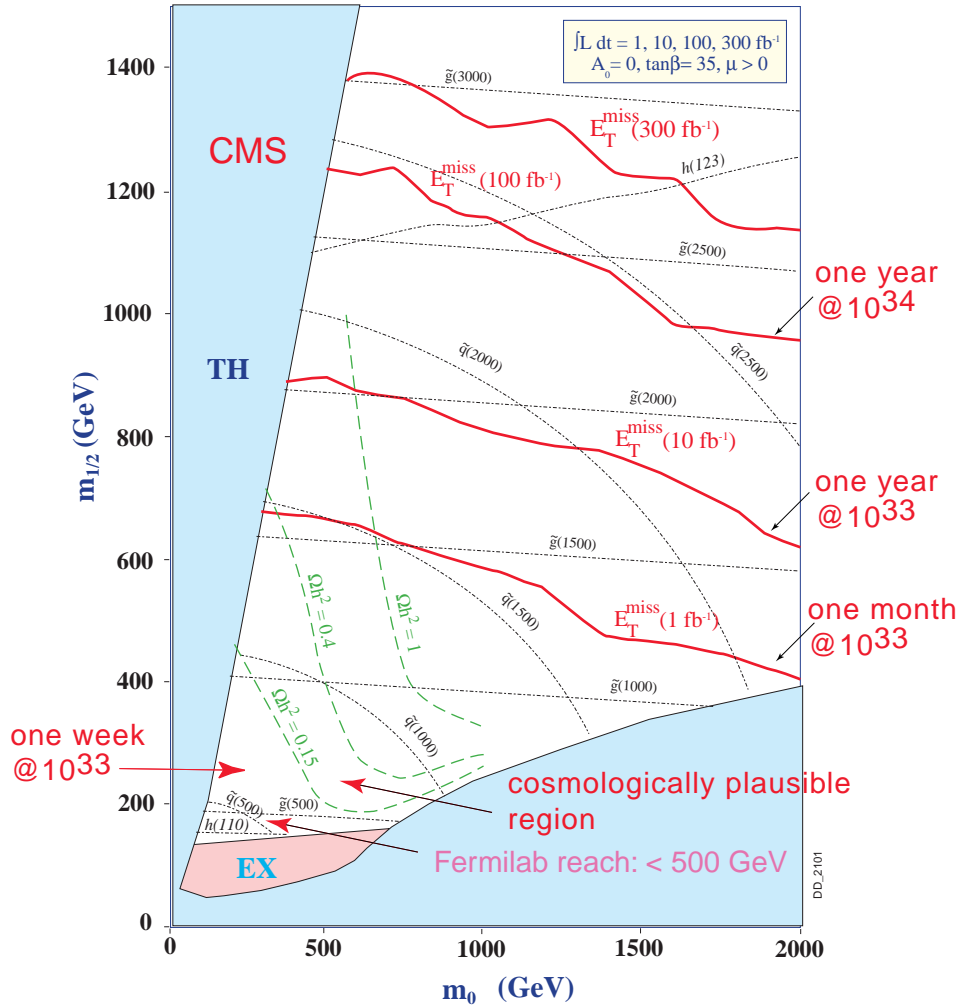


Figure 13. Sketch of the locations of the benchmark points proposed in ⁷⁶ in the region of the $(m_{1/2}, m_0)$ plane where $\Omega_\chi h^2$ falls within the range preferred by cosmology (shaded blue). Note that the filaments of the allowed parameter space extending to large $m_{1/2}$ and/or m_0 are sampled.

supersymmetric Higgs boson would be seen ⁷⁶, as seen in Fig. 16.

Electron-positron colliders provide very clean experimental environments, with egalitarian production of all the new particles that are kinematically accessible, including those that have only weak interactions, and hence are potentially complementary to the LHC, as illustrated in Fig. 16. Moreover, polarized beams provide a useful analysis tool, and $e\gamma$, $\gamma\gamma$ and e^-e^- colliders are readily available at relatively low marginal costs. However, the direct production of supersymmetric particles at such a collider cannot be guaranteed ⁸⁴. We do not yet know what the supersymmetric threshold energy may be (or even if there is one!). We may well not know before the operation of the LHC, although $g_\mu - 2$ might provide an indication ⁷⁰, if the uncertainties in the Standard Model calculation can be reduced. However, if an e^+e^- collider is above the supersymmetric threshold, it will be able to measure very accurately the sparticle masses. By combining its measurements with those made at the LHC, it may be possible to calculate accurately from first principle the supersymmetric relic density and compare it with the astrophysical value.



Catania 18

Figure 14. The regions of the $(m_0, m_{1/2})$ plane that can be explored by the LHC with various integrated luminosities ⁸², using the missing energy + jets signature ⁸¹.

3.6 Searches for Dark Matter Particles

In the above discussion, we have paid particular attention to the region of parameter space where the lightest supersymmetric particle could constitute the cold dark matter in the Universe ⁵⁹. How easy would this be to detect?

- One strategy is to look for relic annihilations in the *galactic halo*, which might

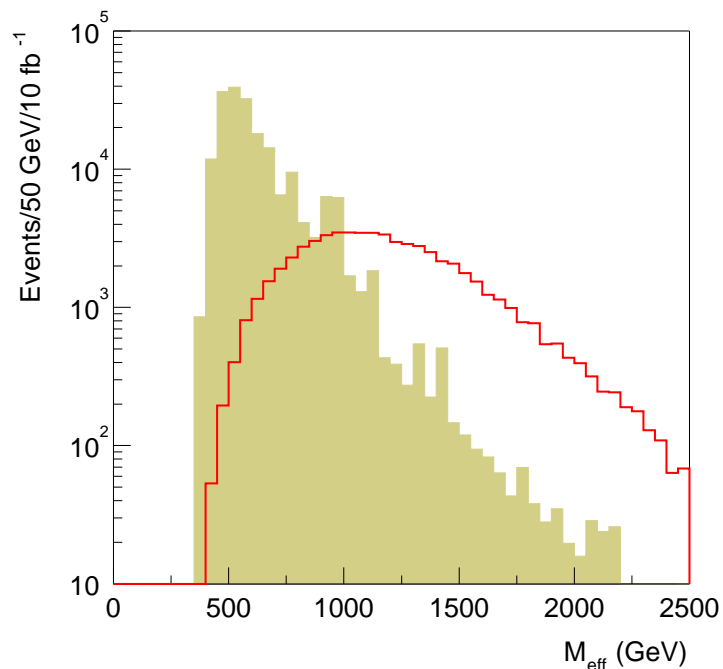


Figure 15. The distribution expected at the LHC in the variable M_{eff} that combines the jet energies with the missing energy ^{83,80,81}.

produce detectable antiprotons or positrons in the cosmic rays ⁸⁵. Unfortunately, the rates for their production are not very promising in the benchmark scenarios we studied ⁸⁶.

- Alternatively, one might look for annihilations in the core of our galaxy, which might produce detectable *gamma rays*. As seen in the left panel of Fig. 17, this may be possible in certain benchmark scenarios ⁸⁶, though the rate is rather uncertain because of the unknown enhancement of relic particles in our galactic core.

- A third strategy is to look for *annihilations inside the Sun or Earth*, where the local density of relic particles is enhanced in a calculable way by scattering off matter, which causes them to lose energy and become gravitationally bound ⁸⁷. The signature would then be energetic neutrinos that might produce detectable muons. Several underwater and ice experiments are underway or planned to look for this signature, and this strategy looks promising for several benchmark scenarios, as seen in the right panel of Fig. 17 ⁸⁶. It will be interesting to have such neutrino telescopes in different hemispheres, which will be able to scan different regions of the sky for astrophysical high-energy neutrino sources.

- The most satisfactory way to look for supersymmetric relic particles is directly

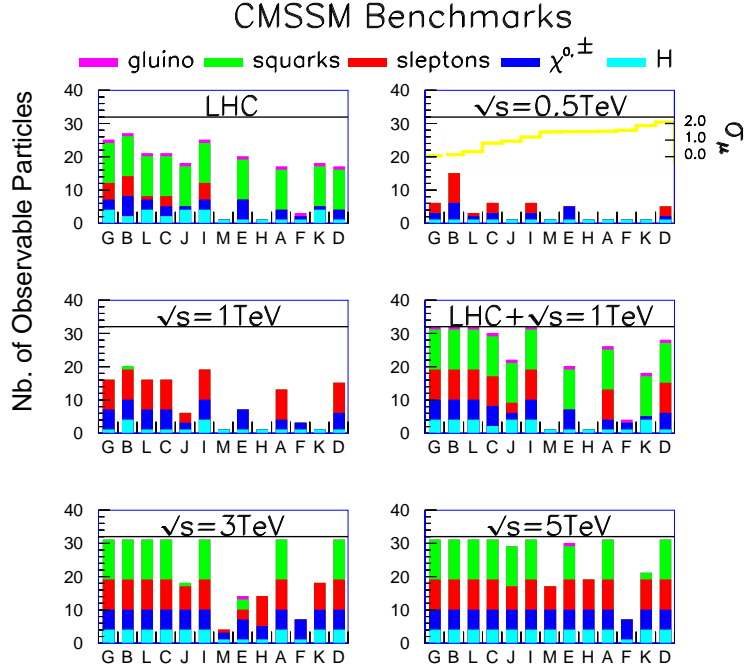


Figure 16. The numbers of different sparticles expected to be observable at the LHC and/or linear e^+e^- colliders with various energies, in each of the proposed benchmark scenarios ⁷⁶, ordered by their difference from the present central experimental value of $g_\mu - 2$ ⁶¹.

via their *elastic scattering on nuclei* in a low-background laboratory experiment ⁸⁸. There are two types of scattering matrix elements, spin-independent - which are normally dominant for heavier nuclei, and spin-dependent - which could be interesting for lighter elements such as fluorine. The best experimental sensitivities so far are for spin-independent scattering, and one experiment has claimed a positive signal ⁸⁹. However, this has not been confirmed by a number of other experiments ⁹⁰. In the benchmark scenarios the rates are considerably below the present experimental sensitivities ⁸⁶, but there are prospects for improving the sensitivity into the interesting range, as seen in Fig. 18.

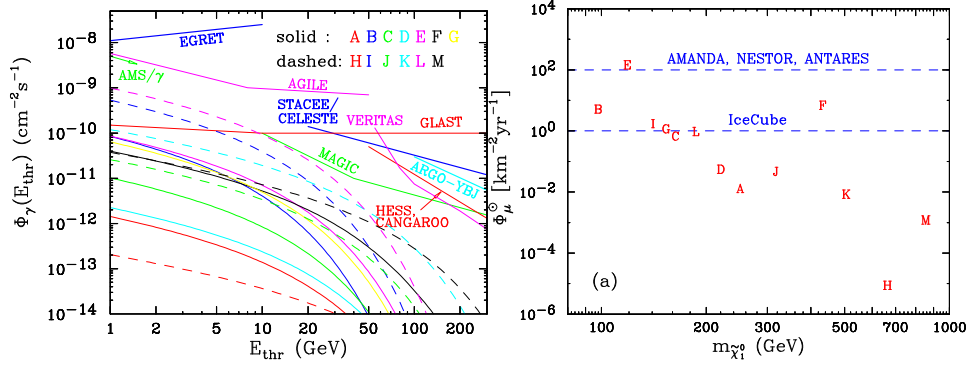


Figure 17. Left panel: Spectra of photons from the annihilations of dark matter particles in the core of our galaxy, in different benchmark supersymmetric models ⁸⁶. Right panel: Signals for muons produced by energetic neutrinos originating from annihilations of dark matter particles in the core of the Sun, in the same benchmark supersymmetric models ⁸⁶.

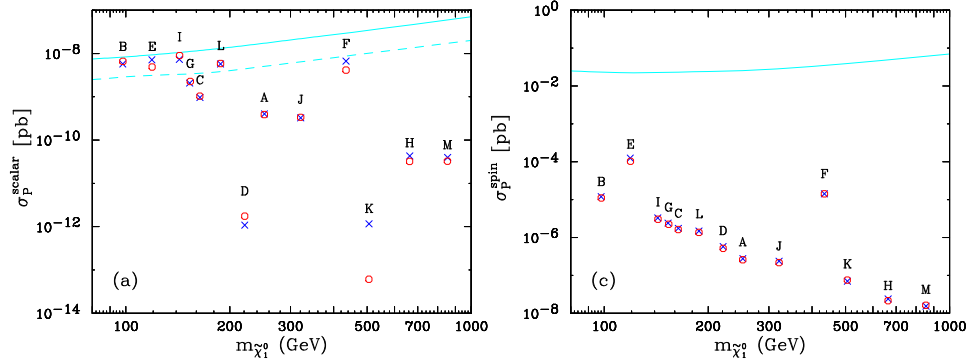


Figure 18. Left panel: elastic spin-independent scattering of supersymmetric relics on protons calculated in benchmark scenarios ⁸⁶, compared with the projected sensitivities for CDMS II ⁹¹ and CRESST ⁹² (solid) and GENIUS ⁹³ (dashed). The predictions of the SSARD code (blue crosses) and Neutdriver ⁹⁴ (red circles) for neutralino-nucleon scattering are compared ⁸⁶. The labels A, B, ...,L correspond to the benchmark points as shown in Fig. 13. Right panel: prospects for detecting elastic spin-dependent scattering in the benchmark scenarios, which are less bright ⁸⁶.

4 Inflation

4.1 Motivations

One of the main motivations for inflation ⁹⁵ is the *horizon* or *homogeneity* problem: why are distant parts of the Universe so similar:

$$\left(\frac{\delta T}{T}\right)_{CMB} \sim 10^{-5} ? \quad (62)$$

In conventional Big Bang cosmology, the largest patch of the CMB sky which could have been causally connected, i.e., across which a signal could have travelled at the speed of light since the initial singularity, is about 2 degrees. So how did opposite parts of the Universe, 180 degrees apart, ‘know’ how to coordinate their temperatures and densities?

Another problem of conventional Big bang cosmology is the *size* or *age* problem. The Hubble expansion rate in conventional Big bang cosmology is given by:

$$H^2 \equiv \left(\frac{\dot{a}}{a}\right)^2 = \frac{8\pi G_N \rho}{3} - \frac{k}{a^2}, \quad (63)$$

where $k = 0$ or ± 1 is the curvature. The only dimensionful coefficient in (63) is the Newton constant, $G_N \equiv 1/M_P^2$: $M_P \simeq 1.2 \times 10^{19}$ GeV. A generic solution of (63) would have a characteristic scale size $a \sim \ell_P \equiv 1/M_P \sim 10^{-33}$ s and live to the ripe old age of $t \sim t_P \equiv \ell_P/c \simeq 10^{-43}$ s. Why is our Universe so long-lived and big? Clearly, we live in an atypical solution of (63)!

A related issue is the *flatness* problem. Defining, as usual

$$\Omega \equiv \frac{\rho}{\rho_c} : \rho_c \equiv \frac{3H^2}{8\pi G_N}, \quad (64)$$

we have

$$\Omega(t) = \frac{1}{1 - \frac{(k/a^2)}{(8\pi G_N \rho/3)}}. \quad (65)$$

Since $\rho \sim a^{-4}$ during the radiation-dominated era and $\sim a^{-3}$ during the matter-dominated era, it is clear from (65) that $\Omega(t) \rightarrow 0$ rapidly: for Ω to be $\mathcal{O}(1)$ as it is today, $|\Omega - 1|$ must have been $\mathcal{O}(10^{-60})$ at the Planck epoch when $t_P \sim 10^{-43}$ s. The density of the very early Universe must have been very finely tuned in order for its geometry to be almost flat today.

Then there is the *entropy* problem: why are there so many particles in the visible Universe: $S \sim 10^{90}$? A ‘typical’ Universe would have contained $\mathcal{O}(1)$ particles in its size $\sim \ell_P^3$.

All these particles have diluted what might have been the primordial density of *unwanted massive particles* such as magnetic monopoles and gravitinos. Where did they go?

The basic idea of inflation⁹⁶ is that, at some early epoch in the history of the Universe, its energy density may have been dominated by an almost constant term:

$$\left(\frac{\dot{a}}{a}\right)^2 = \frac{8\pi G_N \rho}{3} - \frac{k}{a^2} : \rho = V, \quad (66)$$

leading to a phase of almost de Sitter expansion. It is easy to see that the second (curvature) term in (66) rapidly becomes negligible, and that

$$a \simeq a_I e^{Ht} : H = \sqrt{\frac{8\pi G_N}{3} V} \quad (67)$$

during this inflationary expansion.

It is then apparent that the *horizon* would have expanded (near-) exponentially, so that the entire visible Universe might have been within our pre-inflationary horizon. This would have enabled initial homogeneity to have been established. The trick is not somehow to impose connections beyond the horizon, but rather to make the horizon much larger than naively expected in conventional Big Bang cosmology:

$$a_H \simeq a_I e^{H\tau} \gg c\tau, \quad (68)$$

where $H\tau$ is the number of e-foldings during inflation. It is also apparent that the $-\frac{k}{a^2}$ term in (66) becomes negligible, so that the Universe is almost *flat* with $\Omega_{tot} \simeq 1$. However, as we see later, perturbations during inflation generate a small deviation from unity: $|\Omega_{tot} - 1| \simeq 10^{-5}$. Following inflation, the conversion of the inflationary vacuum energy into particles reheats the Universe, filling it with the required *entropy*. Finally, the closest pre-inflationary *monopole* or *gravitino* is pushed away, further than the origin of the CMB, by the exponential expansion of the Universe.

From the point of view of general relativity, the (near-) constant inflationary vacuum energy is equivalent to a cosmological constant Λ :

$$R_{\mu\nu} - \frac{1}{2}g_{\mu\nu}R = 8\pi G_N T_{\mu\nu} + \Lambda g_{\mu\nu}. \quad (69)$$

We may compare the right-hand side of (69) with the energy-momentum tensor of a standard fluid:

$$T_{\mu\nu} = -pg_{\mu\nu} + (\rho + p)U_\mu U_\nu \quad (70)$$

where $U_\mu = (1, 0, 0, 0)$ is the four-momentum vector for a comoving fluid. We can therefore write

$$R_{\mu\nu} - \frac{1}{2}g_{\mu\nu}R = 8\pi G_N T_{\mu\nu}^\Lambda, \quad (71)$$

where

$$\rho_\Lambda \equiv \frac{\Lambda}{8\pi G_N} \equiv -p_\Lambda. \quad (72)$$

Thus, we see that inflation has negative pressure. The value of the cosmological constant today, as suggested by recent observations^{97,98}, is *many* orders of magnitude smaller than would have been required during inflation: $\rho_\Lambda \sim 10^{-50}$ GeV⁴ compared with the density $V \sim 10^{+65}$ GeV⁴ required during inflation, as we see later.

Such a small value of the cosmological energy density is also *much smaller* than many contributions to it from identifiable physics sources: $\rho(QCD) \sim 10^{-4}$ GeV⁴, $\rho(Electroweak) \sim 10^9$ GeV⁴, $\rho(GUT) \sim 10^{64}(?)$ GeV⁴ and $\rho(QuantumGravity) \sim 10^{74}(?)$ GeV⁴. Particle physics offers no reason to expect the present-day vacuum energy to lie within the range suggested by cosmology, and raises the question why it is not many orders of magnitude larger.

4.2 Some Inflationary Models

The first inflationary potential V to be proposed was one with a ‘double-dip’ structure à la Higgs⁹⁶. The *old inflation* idea was that the Universe would have started in the false vacuum with $V \neq 0$, where it would have undergone many e-foldings of de Sitter expansion. Then, the Universe was supposed to have tunneled through the potential barrier to the true vacuum with $V \simeq 0$, and subsequently thermalized. The inflation required before this tunnelling was

$$H\tau \gtrsim 60 : H = \sqrt{\frac{\Lambda}{3}}, \Lambda = 8\pi G_N V. \quad (73)$$

The problem with this old inflationary scenario was that the phase transition to the new vacuum would never have been completed. The Universe would look like a ‘Swiss cheese’ in which the bubbles of true vacuum would be expanding as $t^{1/2}$ or $t^{2/3}$, while the ‘cheese’ between them would still have been expanding exponentially as e^{Ht} . Thus, the fraction of space in the false vacuum would be

$$f \sim \exp \left[Ht \left(3 - \frac{4\pi}{3} \frac{\Gamma}{H^4} \right) \right], \quad (74)$$

where Γ is the bubble nucleation rate per unit four-volume. The fraction $f \rightarrow 0$ only if $\Gamma/H^4 \simeq \mathcal{O}(1)$, but in this case there would not have been sufficient e-foldings for adequate inflation.

One of the fixes for this problem trades under the name of *new inflation*⁹⁹. The idea is that the near-exponential expansion of the Universe took place in a flat region of the potential $V(\phi)$ that is not separated from the true vacuum by any barrier. It might have been reached after a first-order transition of the type postulated in old inflation, in which case one can regard our Universe as part of a bubble that expanded near-exponentially inside the ‘cheese’ of old vacuum, and there could be regions beyond our bubble that are still expanding (near-) exponentially. For the Universe to roll eventually downhill into the true vacuum, $V(\phi)$ could not quite be constant, and hence the Hubble expansion rate H during inflation was also not constant during new inflation.

An example of such a scenario is *chaotic inflation*¹⁰⁰, according to which there is no ‘bump’ in the effective potential $V(\phi)$, and hence no phase transition between old and new vacua. Instead, any given region of the Universe is assumed to start with some random value of the inflaton field ϕ and hence the potential $V(\phi)$, which decreases monotonically to zero. If the initial value of $V(\phi)$ is large enough, and the potential flat enough, (our part of) the Universe will undergo sufficient expansion.

Another fix for old inflation trades under the name of *extended inflation*¹⁰¹. Here the idea is that the tunnelling rate Γ depends on some other scalar field χ that varies while the inflaton ϕ is still stuck in the old vacuum. If $\Gamma(\chi)$ is initially small, but χ then changes so that $\Gamma(\chi)$ becomes large, the problem of completing the transition in the ‘Swiss cheese’ Universe is solved.

All these variants of inflation rely on some type of elementary scalar inflaton field. Therefore, the discovery of a Higgs boson would be a psychological boost for inflation, even though the electroweak Higgs boson cannot be responsible for it directly. Moreover, just as supersymmetry is well suited for stabilizing the mass scale

of the electroweak Higgs boson, it may also be needed to keep the inflationary potential under control¹⁰². Later in this Lecture, I discuss a specific supersymmetric inflationary model.

4.3 Density Perturbations

The above description is quite classical. In fact, one should expect quantum fluctuations in the initial value of the inflaton field ϕ , which would cause the roll-over into the true vacuum to take place inhomogeneously, and different parts of the Universe to expand differently. As we discuss below in more detail, these quantum fluctuations would give rise to a Gaussian random field of perturbations with similar magnitudes on different scale sizes, just as the astrophysicists have long wanted. The magnitudes of these perturbations would be linked to the value of the effective potential during inflation, and would be visible in the CMB as adiabatic temperature fluctuations:

$$\frac{\delta T}{T} \sim \frac{\delta \rho}{\rho} \sim \mu^2 G_N, \quad (75)$$

where $\mu \equiv V^{1/4}$ is a typical vacuum energy scale during inflation. As we discuss later in more detail, consistency with the CMB data from COBE *et al.*, that find $\delta T/T \simeq 10^{-5}$, is obtained if

$$\mu \simeq 10^{16} \text{ GeV}, \quad (76)$$

comparable with the GUT scale.

Each density perturbation can be regarded as an embryonic potential well, into which non-relativistic cold dark matter particles may fall, increasing the local contrast in the mass-energy density. On the other hand, relativistic hot dark matter particles will escape from small-scale density perturbations, modifying their rate of growth. This also depends on the expansion rate of the Universe and hence the cosmological constant. Present-day data are able to distinguish the effects of different categories of dark matter. In particular, as we already discussed, the WMAP and other data tell us that the density of hot dark matter neutrinos is relatively small²⁰:

$$\Omega_\nu h^2 < 0.0076, \quad (77)$$

whereas the density of cold dark matter is relatively large²⁰:

$$\Omega_{CDM} h^2 = 0.1126^{+0.0081}_{-0.0091}, \quad (78)$$

and the cosmological constant is even larger: $\Omega_\Lambda \simeq 0.73$.

The cold dark matter amplifies primordial perturbations already while the conventional baryonic matter is coupled to radiation before (re)combination. Once this epoch is passed and the CMB decouples from the conventional baryonic matter, the baryons become free to fall into the ‘holes’ prepared for them by the cold dark matter that has fallen into the overdense primordial perturbations. In this way, structures in the Universe, such as galaxies and their clusters, may be formed earlier than they would have appeared in the absence of cold dark matter.

All this theory is predicated on the presence of primordial perturbations laid down by inflation ¹⁰³, which we now explore in more detail.

There are in fact two types of perturbations, namely density fluctuations and gravity waves. To describe the first, we consider the density field $\rho(\mathbf{x})$ and its perturbations $\delta(\mathbf{x}) \equiv (\rho(\mathbf{x}) - \langle \rho \rangle) / \langle \rho \rangle$, which we can decompose into Fourier modes:

$$\delta(\mathbf{x}) = \int d^3\mathbf{x} \delta_{\mathbf{k}} e^{-i\mathbf{k}\cdot\mathbf{x}}. \quad (79)$$

The density perturbation on a given scale λ is then given by

$$\left(\frac{\delta\rho}{\rho}\right)_\lambda = \left(\frac{k^3|\delta_{\mathbf{k}}|^2}{2\pi^2}\right)_{k^{-1}=\lambda}, \quad (80)$$

whose evolution depends on the ratio λ/a_H , where $a_H \equiv c \cdot t$ is the naive horizon size.

The evolution of small-scale perturbations with $\lambda/a_H < 1$ depends on the astrophysical dynamics, such as the equation of state, dissipation, the Jeans instability, etc.:

$$\ddot{\delta}_{\mathbf{k}} + 2H\dot{\delta}_{\mathbf{k}} + v_s^2 \frac{k^2}{a^2} \delta_{\mathbf{k}} = 4\pi G_N \langle \rho \rangle \delta_{\mathbf{k}}, \quad (81)$$

where v_s is the sound speed: $v_s^2 = dp/d\rho$. If the wave number k is larger than the characteristic Jeans value

$$k_J = \sqrt{\frac{4\pi G_N a^2 \langle \rho \rangle}{v_s^2}}, \quad (82)$$

the density perturbation $\delta_{\mathbf{k}}$ oscillates, whereas it grows if $k < k_J$. Cold dark matter effectively provides $v_s \rightarrow 0$, in which case $k_J \rightarrow \infty$ and perturbations with all wave numbers grow.

In order to describe the evolution of large-scale perturbations with $\lambda/a_H > 1$, we use the gauge-invariant ratio $\delta\rho/\rho + p$, which remains constant outside the horizon a_H . Hence, the value when such a density perturbation comes back within the horizon is identical with its value when it was inflated beyond the horizon. During inflation, one had $\rho + p \simeq \dot{\phi}^2$, and

$$\delta\rho = \delta\phi \times \frac{\partial V}{\partial\phi} = \delta\phi \times V'(\phi). \quad (83)$$

During roll-over, one has $\ddot{\phi} + 3H\dot{\phi} + V'(\phi) = 0$, and, if the roll-over is slow, one has

$$\dot{\phi} \simeq -\frac{V'(\phi)}{3H}, \quad (84)$$

where the Hubble expansion rate

$$H^2 = \frac{8\pi}{3} G_N \left(V(\phi) + \frac{1}{2} \dot{\phi}^2 \right) \simeq \frac{8\pi G_N}{3} V(\phi). \quad (85)$$

The quantum fluctuations of the inflaton field in de Sitter space are given by:

$$\delta\phi \simeq \frac{H}{2\pi}, \quad (86)$$

so initially

$$\frac{\delta\rho}{\rho+p} \simeq \frac{\delta\phi \cdot V'}{\phi^2} \simeq \frac{H^3 \cdot V'}{(V')^2} \simeq \frac{V^{3/2}}{V'}. \quad (87)$$

This is therefore also the value when the perturbation comes back within the horizon:

$$\left(\frac{\delta\rho}{\rho}\right)_{\lambda=a_H} \equiv A_S(\phi) = \frac{\sqrt{2}\kappa^2 H^2}{8\pi^{3/2} |H'|} : \quad \kappa^2 \equiv 8\pi G_N, \quad (88)$$

assuming that $\rho \gg p$ at this epoch.

Gravity-wave perturbations obey an equation analogous to (81):

$$\ddot{h}_{\mathbf{k}}^{1,2} + 2H\dot{h}_{\mathbf{k}}^{1,2} + v_s^2 \frac{k^2}{a^2} h_{\mathbf{k}}^{1,2} = 0, \quad (89)$$

for each of the two graviton polarization states $h_{\mu\nu}^{1,2}$, where

$$g_{\mu\nu} = g_{\mu\nu}^{FRW} + h_{\mu\nu}. \quad (90)$$

The $h_{\mathbf{k}}^{1,2}$ also remain unchanged outside the horizon a_H , and have initial values

$$h_{\mathbf{k}}^{1,2} \simeq \frac{H}{2\pi}, \quad (91)$$

yielding

$$k^3 |h_{\mathbf{k}}|_{\lambda=a_H} \equiv A_T(\phi) = \frac{\kappa}{4\pi^{3/2}} H : \quad H \simeq \sqrt{\frac{8\pi G_N}{3}} V. \quad (92)$$

Comparing (88, 92), we see that

$$r \equiv \frac{A_S(\phi)}{A_T(\phi)} = \frac{\kappa}{\sqrt{2}} \frac{H}{|H'|} : \quad \kappa^2 = 8\pi G_N. \quad (93)$$

Hence, if the roll-over is very slow, so that $|H'|$ is very small, the density waves dominate over the tensor gravity waves. However, in the real world, also the gravity waves may be observable, furnishing a possible signature of inflation ¹⁰⁴.

4.4 Inflation in Scalar Field Theories

Let now consider in more detail chaotic inflation in a generic scalar field theory ¹⁰⁴, described by a Lagrangian

$$\mathcal{L}(\phi) = \frac{1}{2} \partial^\mu \phi \partial_\mu \phi - V(\phi), \quad (94)$$

where the first term yields the kinetic energy of the inflaton field ϕ and the second term is the inflaton potential. One may treat the inflaton field as a fluid with density

$$\rho = \frac{1}{2} \dot{\phi}^2 + V(\phi), \quad (95)$$

and pressure

$$p = \frac{1}{2}\dot{\phi}^2 - V(\phi). \quad (96)$$

Inserting these expressions into the standard FRW equations, we find that the Hubble expansion rate is given by

$$H^2 = \frac{8\pi}{3\pi^2} \left[\frac{1}{2}\dot{\phi}^2 + V(\phi) \right], \quad (97)$$

as discussed above, the deceleration rate is given by

$$\left(\frac{\ddot{a}}{a} \right) = \frac{8\pi}{3\pi^2} \left[V(\phi) - \frac{1}{2}\dot{\phi}^2 \right], \quad (98)$$

and the equation of motion of the inflaton field is

$$\ddot{\phi} + 3H\dot{\phi} + V'(\phi) = 0. \quad (99)$$

The first term in (99) is assumed to be negligible, in which case the equation of motion is dominated by the second (Hubble drag) term, and one has

$$\dot{\phi} \simeq -\frac{V'}{3H}, \quad (100)$$

as assumed above. In this slow-roll approximation, when the kinetic term in (97) is negligible, and the Hubble expansion rate is dominated by the potential term:

$$H \simeq \sqrt{\frac{1}{3M_P^2}V(\phi)}. \quad (101)$$

where $M_P \equiv 1/\sqrt{8\pi G_N} \simeq 2.4 \times 10^{18}$ GeV. It is convenient to introduce the following slow-roll parameters:

$$\epsilon \equiv \frac{1}{2}M_P^2 \left(\frac{V'}{V} \right)^2, \quad \eta \equiv M_P^2 \left(\frac{V''}{V} \right), \quad \xi \equiv M_P^4 \left(\frac{VV'''}{V^2} \right). \quad (102)$$

Various observable quantities can then be expressed in terms of ϵ , η and ξ , including the spectral index for scalar density perturbations:

$$n_s = 1 - 6\epsilon + 2\eta, \quad (103)$$

the ratio of scalar and tensor perturbations at the quadrupole scale:

$$r \equiv \frac{A_T}{A_S} = 16\epsilon, \quad (104)$$

the spectral index of the tensor perturbations:

$$n_T = -2\epsilon, \quad (105)$$

and the running parameter for the scalar spectral index:

$$\frac{dn_s}{d\ln k} = \frac{2}{3} \left[(n_s - 1)^2 - 4\eta^2 \right] + 2\xi. \quad (106)$$

The amount e^N by which the Universe expanded during inflation is also controlled by the slow-roll parameter ϵ :

$$e^N : N = \int H dt = \frac{2\sqrt{\pi}}{m_P} \int_{\phi_{initial}}^{\phi_{final}} \frac{d\phi}{\sqrt{\epsilon(\phi)}}. \quad (107)$$

In order to explain the size of a feature in the observed Universe, one needs:

$$N = 62 - \ln \frac{k}{a_0 H_0} - \ln \frac{10^{16} \text{GeV}}{V_k^{1/4}} + \frac{1}{4} \ln \frac{V_k}{V_e} - \frac{1}{3} \ln \frac{V_e^{1/4}}{\rho_{reheating}^{1/4}}, \quad (108)$$

where k characterizes the size of the feature, V_k is the magnitude of the inflaton potential when the feature left the horizon, V_e is the magnitude of the inflaton potential at the end of inflation, and $\rho_{reheating}$ is the density of the Universe immediately following reheating after inflation.

As an example of the above general slow-roll theory, let us consider chaotic inflation¹⁰⁰ with a $V = \frac{1}{2}m^2\phi^2$ potential^a, and compare its predictions with the WMAP data²⁰. In this model, the conventional slow-roll inflationary parameters are

$$\epsilon = \frac{2M_P^2}{\phi_I^2}, \quad \eta = \frac{2M_P^2}{\phi_I^2}, \quad \xi = 0, \quad (109)$$

where ϕ_I denotes the *a priori* unknown inflaton field value during inflation at a typical CMB scale k . The overall scale of the inflationary potential is normalized by the WMAP data on density fluctuations:

$$\Delta_R^2 = \frac{V}{24\pi^2 M_P^2 \epsilon} = 2.95 \times 10^{-9} A \quad : \quad A = 0.77 \pm 0.07, \quad (110)$$

yielding

$$V^{\frac{1}{4}} = M_P^4 \sqrt{\epsilon \times 24\pi^2 \times 2.27 \times 10^{-9}} = 0.027 M_P \times \epsilon^{\frac{1}{4}}, \quad (111)$$

corresponding to

$$m^{\frac{1}{2}} \phi_I = 0.038 \times M_P^{\frac{3}{2}} \quad (112)$$

in any simple chaotic ϕ^2 inflationary model. The above expression (108) for the number of e-foldings after the generation of the CMB density fluctuations observed by COBE could be as low as $N \simeq 50$ for a reheating temperature T_{RH} as low as 10^6 GeV. In the ϕ^2 inflationary model, this value of N would imply

$$N = \frac{1}{4} \frac{\phi_I^2}{M_P^2} \simeq 50, \quad (113)$$

corresponding to

$$\phi_I^2 \simeq 200 \times M_P^2. \quad (114)$$

^aThis is motivated by the sneutrino inflation model¹⁰⁵ discussed later.

Inserting this requirement into the WMAP normalization condition (111), we find the following required mass for any quadratic inflaton:

$$m \simeq 1.8 \times 10^{13} \text{ GeV}. \quad (115)$$

This is comfortably within the range of heavy singlet (s)neutrino masses usually considered, namely $m_N \sim 10^{10}$ to 10^{15} GeV, motivating the sneutrino inflation model ¹⁰⁵ discussed below.

Is this simple ϕ^2 model compatible with the WMAP data? It predicts the following values for the primary CMB observables ¹⁰⁵: the scalar spectral index

$$n_s = 1 - \frac{8M_P^2}{\phi_I^2} \simeq 0.96, \quad (116)$$

the tensor-to scalar ratio

$$r = \frac{32M_P^2}{\phi_I^2} \simeq 0.16, \quad (117)$$

and the running parameter for the scalar spectral index:

$$\frac{dn_s}{d\ln k} = \frac{32M_P^4}{\phi_I^4} \simeq 8 \times 10^{-4}. \quad (118)$$

The value of n_s extracted from WMAP data depends whether, for example, one combines them with other CMB and/or large-scale structure data. However, the ϕ^2 model value $n_s \simeq 0.96$ appears to be compatible with the data at the 1- σ level. The ϕ^2 model value $r \simeq 0.16$ for the relative tensor strength is also compatible with the WMAP data. In fact, we note that the favoured individual values for n_s, r and $dn_s/d\ln k$ reported in an independent analysis ¹⁰⁶ *all coincide* with the ϕ^2 model values, within the latter's errors!

One of the most interesting features of the WMAP analysis is the possibility that $dn_s/d\ln k$ might differ from zero. The ϕ^2 model value $dn_s/d\ln k \simeq 8 \times 10^{-4}$ derived above is negligible compared with the WMAP preferred value and its uncertainties. However, $dn_s/d\ln k = 0$ appears to be compatible with the WMAP analysis at the 2- σ level or better, so we do not regard this as a death-knell for the ϕ^2 model.

4.5 *Could the Inflaton be a Sneutrino?*

This 'old' idea ¹⁰⁷ has recently been resurrected ¹⁰⁵. We recall that seesaw models ²⁵ of neutrino masses involve three heavy singlet right-handed neutrinos weighing around 10^{10} to 10^{15} GeV, which certainly includes the preferred inflaton mass found above (115). Moreover, supersymmetry requires each of the heavy neutrinos to be accompanied by scalar sneutrino partners. In addition, singlet (s)neutrinos have no interactions with vector bosons, so their effective potential may be as flat as one could wish. Moreover, supersymmetry safeguards the flatness of this potential against radiative corrections. Thus, singlet sneutrinos have no problem in meeting the slow-roll requirements of inflation.

On the other hand, their Yukawa interactions Y_D are eminently suitable for converting the inflaton energy density into particles via $N \rightarrow H + \ell$ decays and

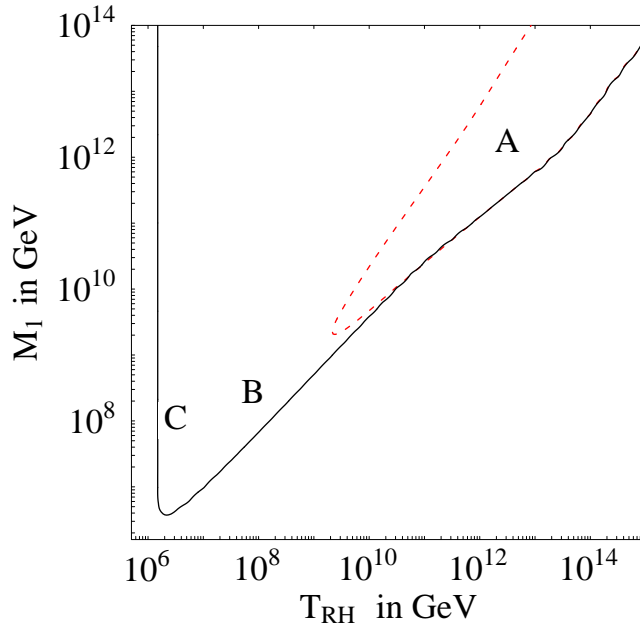


Figure 19. The solid curve bounds the region allowed for leptogenesis in the (T_{RH}, M_{N_1}) plane, assuming a baryon-to-entropy ratio $Y_B > 7.8 \times 10^{-11}$ and the maximal CP asymmetry $\epsilon_1^{max}(M_{N_1})$. In the area bounded by the red dashed curve leptogenesis is entirely thermal ¹⁰⁵.

their supersymmetric variants. Since the magnitudes of these Yukawa interactions are not completely determined, there is flexibility in the reheating temperature after inflation, as we see in Fig. 19 ¹⁰⁵. Thus the answer to the question in the title of this Section seems to be ‘yes’, so far.

5 Further Beyond

Some key cosmological and astrophysical problems may be resolved only by appeal to particle physics beyond the ideas we have discussed so far. One of the greatest successes of Big Bang cosmology has been an explanation of the observed abundances of light elements, ascribed to cosmological nucleosynthesis when the temperature $T \sim 1$ to 0.1 MeV. This requires a small baryon-to-entropy ratio $n_B/s \simeq 10^{-10}$. How did this small baryon density originate?

Looking back to the previous quark epoch, there must have been a small excess of quarks over antiquarks. All the antiquarks would then have annihilated with quarks when the temperature of the Universe was ~ 200 MeV, producing radiation and leaving the small excess of quarks to survive to form baryons. So how did the

small excess of quarks originate?

Sakharov¹⁰⁸ pointed out that microphysics, in the form of particle interactions, could generate a small excess of quarks if the following three conditions were satisfied:

- *The interactions of matter and antimatter particles should differ*, in the sense that both charge conjugation C and its combination CP with mirror reflection should be broken, as discovered in the weak interactions.

- *There should exist interactions capable of changing the net quark number*. Such interactions do exist in the Standard Model, mediated by unstable field configurations called sphalerons. They have not been observed at low temperatures, where they would be mediated by heavy states called sphalerons and are expected to be very weak, but they are thought to have been important when the temperature of the Universe was $\gtrsim 100$ GeV. Alternatively, one may appeal to interactions in Grand Unified Theories (GUTs) that are thought to change quarks into leptons and *vice versa* when their energies $\sim 10^{15}$ GeV.

- *There should have been a breakdown of thermal equilibrium*. This could have occurred during a phase transition in the early Universe, for example during the electroweak phase transition when $T \sim 100$ GeV, during inflation, or during a GUT phase transition when $T \sim 10^{15}$ GeV.

The great hope in the business of cosmological baryogenesis is to find a connection with physics accessible to accelerator experiments, and some examples will be mentioned later in this Lecture.

Another example of observable phenomena related to GUT physics may be ultra-high-energy cosmic rays (UHECRs)¹⁰⁹, which have energies $\gtrsim 10^{11}$ GeV. The UHECRs might either have originated from some astrophysical source, such as an active galactic nuclei (AGNs) or gamma-ray bursters (GRBs), or they might be due to the decays of metastable GUT-scale particles, a possibility discussed in the last part of this Lecture.

5.1 Grand Unified Theories

The philosophy of grand unification¹¹⁰ is to seek a simple group that includes the untidy separate interactions of the Standard Model, QCD and the electroweak sector. The hope is that this Grand Unification can be achieved while neglecting gravity, at least as a first approximation. If the grand unification scale turns out to be significantly less than the Planck mass, this is not obviously a false hope. The Grand Unification scale is indeed expected to be exponentially large:

$$\frac{m_{GUT}}{m_W} = \exp\left(\mathcal{O}\left(\frac{1}{\alpha_{em}}\right)\right) \quad (119)$$

and typical estimates are that $m_{GUT} = \mathcal{O}(10^{16}$ GeV). Such a calculation involves an extrapolation of known physics by many orders of magnitude further than, e.g., the extrapolation that Newton made from the apple to the Solar System.

If the grand unification scale is indeed so large, most tests of it are likely to be indirect, such as relations between Standard Model vector couplings and between particle masses. Any new interactions, such as those that might cause protons to

decay or give masses to neutrinos, are likely to be very strongly suppressed.

To examine the indirect GUT predictions for the Standard Model vector interactions in more detail, one needs to study their variations with the energy scale ⁵⁷, which are described by the following two-loop renormalization equations:

$$Q \frac{\partial \alpha_i(Q)}{\partial Q} = -\frac{1}{2\pi} \left(b_i + \frac{b_{ij}}{4\pi} \alpha_j(Q) \right) [\alpha_i(Q)]^2 \quad (120)$$

where the b_i receive the one-loop contributions

$$b_i = \begin{pmatrix} 0 \\ -\frac{22}{3} \\ -11 \end{pmatrix} + N_g \begin{pmatrix} \frac{4}{3} \\ \frac{4}{3} \\ \frac{4}{3} \end{pmatrix} + N_H \begin{pmatrix} \frac{1}{10} \\ \frac{1}{6} \\ 0 \end{pmatrix} \quad (121)$$

from vector bosons, N_g matter generations and N_H Higgs doublets, respectively, and at two loops

$$b_{ij} = \begin{pmatrix} 0 & 0 & 0 \\ 0 & -\frac{136}{3} & 0 \\ 0 & 0 & -102 \end{pmatrix} + N_g \begin{pmatrix} \frac{19}{15} & \frac{3}{5} & \frac{44}{15} \\ \frac{1}{5} & \frac{49}{3} & 4 \\ \frac{4}{30} & \frac{3}{2} & \frac{76}{3} \end{pmatrix} + N_H \begin{pmatrix} \frac{9}{50} & \frac{9}{10} & 0 \\ \frac{3}{10} & \frac{13}{6} & 0 \\ 0 & 0 & 0 \end{pmatrix}. \quad (122)$$

These coefficients are all independent of any specific GUT model, depending only on the light particles contributing to the renormalization.

Including supersymmetric particles as in the MSSM, one finds ¹¹¹

$$b_i = \begin{pmatrix} 0 \\ -6 \\ -9 \end{pmatrix} + N_g \begin{pmatrix} 2 \\ 2 \\ 2 \end{pmatrix} + N_H \begin{pmatrix} \frac{3}{10} \\ \frac{1}{2} \\ 0 \end{pmatrix} \quad (123)$$

and

$$b_{ij} = \begin{pmatrix} 0 & 0 & 0 \\ 0 & -24 & 0 \\ 0 & 0 & -54 \end{pmatrix} + N_g \begin{pmatrix} \frac{38}{15} & \frac{6}{5} & \frac{88}{15} \\ \frac{2}{5} & 14 & 8 \\ \frac{11}{5} & 3 & \frac{68}{3} \end{pmatrix} + N_H \begin{pmatrix} \frac{9}{50} & \frac{9}{10} & 0 \\ \frac{3}{10} & \frac{7}{2} & 0 \\ 0 & 0 & 0 \end{pmatrix}, \quad (124)$$

again independent of any specific supersymmetric GUT.

Calculations with these equations show that non-supersymmetric models are not consistent with the measurements of the Standard Model interactions at LEP and elsewhere. However, although extrapolating the experimental determinations of the interaction strengths using the non-supersymmetric renormalization-group equations (121), (122) does not lead to a common value at any renormalization scale, we saw in Fig. 11 that extrapolation using the supersymmetric equations (123), (124) **does** lead to possible unification at $m_{GUT} \sim 10^{16}$ GeV ⁵⁶.

The simplest GUT model is based on the group SU(5) ¹¹⁰, whose most useful representations are the complex vector $\underline{5}$ representation denoted by F_α , its conjugate

$\underline{\bar{5}}$ denoted by \bar{F}^α , the complex two-index antisymmetric tensor $\underline{10}$ representation $T_{[\alpha\beta]}$, and the adjoint $\underline{24}$ representation A_β^α . The latter is used to accommodate the vector bosons of SU(5):

$$\left(\begin{array}{cccc} & & & \vdots \quad \bar{X} \quad \bar{Y} \\ & & & \vdots \quad \bar{X} \quad \bar{Y} \\ & g_{1,\dots,8} & & \vdots \quad \bar{X} \quad \bar{Y} \\ & & & \vdots \quad \bar{X} \quad \bar{Y} \\ \dots & & & \dots \\ X & X & X & \vdots \\ & & & \vdots \quad W_{1,2,3} \\ Y & Y & Y & \vdots \end{array} \right) \quad (125)$$

where the $g_{1,\dots,8}$ are the gluons of QCD, the $W_{1,2,3}$ are weak bosons, and the (X, Y) are new vector bosons, whose interactions we discuss in the next section.

The quarks and leptons of each generation are accommodated in $\underline{\bar{5}}$ and $\underline{10}$ representations of SU(5):

$$\bar{F} = \left(\begin{array}{c} d_R^c \\ d_Y^c \\ d_B^c \\ \dots \\ -e^- \\ \nu_e \end{array} \right)_L, \quad T = \left(\begin{array}{cccccc} 0 & u_B^c & -u_Y^c & \vdots & -u_R & -d_R \\ -u_B^c & 0 & u_R^c & \vdots & -u_Y & -d_Y \\ u_Y^c & -u_R^c & 0 & \vdots & -u_B & -d_B \\ \dots & & & \dots & & \\ u_R & u_Y & u_B & \vdots & 0 & -e^c \\ d_R & d_Y & d_B & \vdots & e^c & 0 \end{array} \right)_L \quad (126)$$

The particle assignments are unique up to the effects of mixing between generations, which we do not discuss in detail here ¹¹².

5.2 Baryon Decay and Baryogenesis

Baryon instability is to be expected on general grounds, since there is no exact symmetry to guarantee that baryon number B is conserved, just as we discussed previously for lepton number. Indeed, baryon decay is a generic prediction of GUTs, which we illustrate with the simplest SU(5) model. We see in (125) that there are two species of vector bosons in SU(5) that couple the colour indices (1,2,3) to the electroweak indices (4,5), called X and Y . As we can see from the matter representations (126), these may enable two quarks or a quark and lepton to annihilate. Combining these possibilities leads to interactions with $\Delta B = \Delta L = 1$. The forms of effective four-fermion interactions mediated by the exchanges of massive Z and Y bosons, respectively, are ¹¹³:

$$\begin{aligned} & (\epsilon_{ijk} u_{R_k} \gamma_\mu u_{L_j}) \frac{g_X^2}{8m_X^2} (2e_R \gamma^\mu d_{L_i} + e_L \gamma^\mu d_{R_i}), \\ & (\epsilon_{ijk} u_{R_k} \gamma_\mu d_{L_j}) \frac{g_Y^2}{8m_X^2} (\nu_L \gamma^\mu d_{R_i}), \end{aligned} \quad (127)$$

up to generation mixing factors.

Since the couplings $g_X = g_Y$ in an SU(5) GUT, and $m_X \simeq m_Y$, we expect that

$$G_X \equiv \frac{g_X^2}{8m_X^2} \simeq G_Y \equiv \frac{g_Y^2}{8m_Y^2}. \quad (128)$$

It is clear from (127) that the baryon decay amplitude $A \propto G_X$, and hence the baryon $B \rightarrow \ell +$ meson decay rate

$$\Gamma_B = cG_X^2 m_p^5, \quad (129)$$

where the factor of m_p^5 comes from dimensional analysis, and c is a coefficient that depends on the GUT model and the non-perturbative properties of the baryon and meson.

The decay rate (129) corresponds to a proton lifetime

$$\tau_p = \frac{1}{c} \frac{m_X^4}{m_p^5}. \quad (130)$$

It is clear from (130) that the proton lifetime is very sensitive to m_X , which must therefore be calculated very precisely. In minimal SU(5), the best estimate was

$$m_X \simeq (1 \text{ to } 2) \times 10^{15} \times \Lambda_{QCD} \quad (131)$$

where Λ_{QCD} is the characteristic QCD scale. Making an analysis of the generation mixing factors¹¹², one finds that the preferred proton (and bound neutron) decay modes in minimal SU(5) are

$$\begin{aligned} p &\rightarrow e^+ \pi^0, \quad e^+ \omega, \quad \bar{\nu} \pi^+, \quad \mu^+ K^0, \quad \dots \\ n &\rightarrow e^+ \pi^-, \quad e^+ \rho^-, \quad \bar{\nu} \pi^0, \quad \dots \end{aligned} \quad (132)$$

and the best numerical estimate of the lifetime is

$$\tau(p \rightarrow e^+ \pi^0) \simeq 2 \times 10^{31 \pm 1} \times \left(\frac{\Lambda_{QCD}}{400 \text{ MeV}} \right)^4 \text{ y} \quad (133)$$

This is in *prima facie* conflict with the latest experimental lower limit

$$\tau(p \rightarrow e^+ \pi^0) > 1.6 \times 10^{33} \text{ y} \quad (134)$$

from super-Kamiokande¹¹⁴.

We saw earlier that supersymmetric GUTs, including SU(5), fare better with coupling unification. They also predict a larger GUT scale¹¹¹:

$$m_X \simeq 10^{16} \text{ GeV}, \quad (135)$$

so that $\tau(p \rightarrow e^+ \pi^0)$ is considerably longer than the experimental lower limit. However, this is not the dominant proton decay mode in supersymmetric SU(5)¹¹⁵. In this model, there are important $\Delta B = \Delta L = 1$ interactions mediated by the exchange of colour-triplet Higgsinos \tilde{H}_3 , dressed by gaugino exchange¹¹⁶:

$$G_X \rightarrow \mathcal{O} \left(\frac{\lambda^2 g^2}{16\pi^2} \right) \frac{1}{m_{\tilde{H}_3} \tilde{m}} \quad (136)$$

where λ is a Yukawa coupling. Taking into account colour factors and the increase in λ for more massive particles, it was found¹¹⁵ that decays into neutrinos and strange particles should dominate:

$$p \rightarrow \bar{\nu}K^+, \quad n \rightarrow \bar{\nu}K^0, \quad \dots \quad (137)$$

Because there is only one factor of a heavy mass $m_{\tilde{H}_3}$ in the denominator of (136), these decay modes are expected to dominate over $p \rightarrow e^+\pi^0$, etc., in minimal supersymmetric SU(5). Calculating carefully the other factors in (136)¹¹⁵, it seems that the modes (137) may now be close to exclusion at rates compatible with this model. The current experimental limit is $\tau(p \rightarrow \bar{\nu}K^+) > 6.7 \times 10^{32}y$. However, there are other GUT models²⁸ that remain compatible with the baryon decay limits.

The presence of baryon-number-violating interactions opens the way to cosmological baryogenesis via the out-of-equilibrium decays of GUT bosons¹¹⁷:

$$X \rightarrow q + \bar{\ell} \quad vs \quad \bar{X} \rightarrow \bar{q} + \ell. \quad (138)$$

In the presence of C and CP violation, the branching ratios for $X \rightarrow q + \bar{\ell}$ and $\bar{X} \rightarrow \bar{q} + \ell$ may differ. Such a difference may in principle be generated by quantum (loop) corrections to the leading-order interactions of GUT bosons. This effect is too small in the minimal SU(5) GUT described above¹¹⁸, but could be larger in some more complicated GUT. One snag is that, with GUT bosons as heavy as suggested above, the CP-violating decay asymmetry may tend to get washed out by thermal effects. This difficulty may in principle be avoided by appealing to the decays of GUT Higgs bosons, which might weigh $\ll 10^{15}$ GeV, though this possibility is not strongly motivated.

Although neutrino masses might arise without a GUT framework, they appear very naturally in most GUTs, and this framework helps motivated the mass scale $\sim 10^{10}$ to 10^{15} GeV required for the heavy singlet neutrinos. Their decays provide an alternative mechanism for generating the baryon asymmetry of the Universe, namely leptogenesis⁴⁹. In the presence of C and CP violation, the branching ratios for $N \rightarrow \text{Higgs} + \ell$ may differ from that for $N \rightarrow \text{Higgs} + \bar{\ell}$, producing a net lepton asymmetry. The likely masses for heavy singlet neutrinos could be significantly lower than the GUT scale, so it may be easier to avoid thermal washout effects. However, you may ask what is the point of generating a lepton asymmetry, since we want a quark asymmetry? The answer is provided by the weak sphaleron interactions that are present in the Standard Model, and would have converted part of the lepton asymmetry into the desired quark asymmetry. We now discuss how this scenario might have operated in the minimal seesaw model for neutrino masses discussed in Lecture 2.

5.3 Leptogenesis in the Seesaw Model

As mentioned in the second Lecture, the minimal seesaw neutrino model contains 18 parameters⁴⁴, of which only 9 are observable in low-energy neutrino interactions: 3 light neutrino masses, 3 real mixing angles $\theta_{12,23,31}$, the oscillation phase δ and the 2 Majorana phases $\phi_{1,2}$.

To see how the extra 9 parameters appear ⁴⁵, we reconsider the full lepton sector, assuming that we have diagonalized the charged-lepton mass matrix:

$$(Y_\ell)_{ij} = Y_{\ell_i}^d \delta_{ij}, \quad (139)$$

as well as that of the heavy singlet neutrinos:

$$M_{ij} = M_i^d \delta_{ij}. \quad (140)$$

We can then parametrize the neutrino Dirac coupling matrix Y_ν in terms of its real and diagonal eigenvalues and unitary rotation matrices:

$$Y_\nu = Z^* Y_{\nu_k}^d X^\dagger, \quad (141)$$

where X has 3 mixing angles and one CP-violating phase, just like the CKM matrix, and we can write Z in the form

$$Z = P_1 \bar{Z} P_2, \quad (142)$$

where \bar{Z} also resembles the CKM matrix, with 3 mixing angles and one CP-violating phase, and the diagonal matrices $P_{1,2}$ each have two CP-violating phases:

$$P_{1,2} = \text{Diag} (e^{i\theta_{1,3}}, e^{i\theta_{2,4}}, 1). \quad (143)$$

In this parametrization, we see explicitly that the neutrino sector has 18 parameters ⁴⁴: the 3 heavy-neutrino mass eigenvalues M_i^d , the 3 real eigenvalues of $Y_{\nu_i}^D$, the 6 = 3 + 3 real mixing angles in X and \bar{Z} , and the 6 = 1 + 5 CP-violating phases in X and \bar{Z} ⁴⁵.

The total decay rate of a heavy neutrino N_i may be written in the form

$$\Gamma_i = \frac{1}{8\pi} (Y_\nu Y_\nu^\dagger)_{ii} M_i. \quad (144)$$

One-loop CP-violating diagrams involving the exchange of heavy neutrino N_j would generate an asymmetry in N_i decay of the form:

$$\epsilon_{ij} = \frac{1}{8\pi} \frac{1}{(Y_\nu Y_\nu^\dagger)_{ii}} \text{Im} \left((Y_\nu Y_\nu^\dagger)_{ij} \right)^2 f \left(\frac{M_j}{M_i} \right), \quad (145)$$

where $f(M_j/M_i)$ is a known kinematic function.

Thus we see that leptogenesis ⁴⁹ is proportional to the product

$$Y_\nu Y_\nu^\dagger = P_1^* \bar{Z}^* (Y_\nu^d)^2 \bar{Z}^T P_1, \quad (146)$$

which depends on 13 of the real parameters and 3 CP-violating phases. As mentioned in Lecture 2, the extra seesaw parameters also contribute to the renormalization of soft supersymmetry-breaking masses, in leading order via the combination

$$Y_\nu^\dagger Y_\nu = X (Y_\nu^d)^2 X^\dagger, \quad (147)$$

which depends on just 1 CP-violating phase, with two more phases appearing in higher orders, when one allows the heavy singlet neutrinos to be non-degenerate ⁴⁷.

In order to see how the low-energy sector is embedded in the full parametrization of the seesaw model, and hence its (lack of) relation to leptogenesis ⁵⁰, we first recall

that the 3 phases in \tilde{P}_2 (46) become observable when one also considers high-energy quantities. Next, we introduce a complex orthogonal matrix

$$R \equiv \sqrt{M^d}^{-1} Y_\nu U \sqrt{M^d}^{-1} [v \sin \beta], \quad (148)$$

which has 3 real mixing angles and 3 phases: $R^T R = 1$. These 6 additional parameters may be used to characterize Y_ν , by inverting

$$Y_\nu = \frac{\sqrt{M^d} R \sqrt{M^d} U^\dagger}{[v \sin \beta]}, \quad (149)$$

giving us the grand total of $18 = 9 + 3 + 6$ parameters⁴⁵. The leptogenesis observable (146) may now be written in the form

$$Y_\nu Y_\nu^\dagger = \frac{\sqrt{M^d} R \mathcal{M}_\nu^d R^\dagger \sqrt{M^d}}{[v^2 \sin^2 \beta]}, \quad (150)$$

which depends on the 3 phases in R , but *not* the 3 low-energy phases $\delta, \phi_{1,2}$, *nor* the 3 real MNS mixing angles⁴⁵!

The basic reason for this is that one makes a unitary sum over all the light lepton species in evaluating the asymmetry ϵ_{ij} . It is easy to derive a compact expression for ϵ_{ij} in terms of the heavy neutrino masses and the complex orthogonal matrix R :

$$\epsilon_{ij} = \frac{1}{8\pi} M_j f \left(\frac{M_j}{M_i} \right) \frac{\text{Im} \left((R \mathcal{M}_\nu^d R^\dagger)_{ij} \right)^2}{(R \mathcal{M}_\nu^d R^\dagger)_{ii}}, \quad (151)$$

which depends explicitly on the extra phases in R . How can we measure them?

In general, one may formulate the following strategy for calculating leptogenesis in terms of laboratory observables^{45,50}:

- Measure the neutrino oscillation phase δ and the Majorana phases $\phi_{1,2}$,
- Measure observables related to the renormalization of soft supersymmetry-breaking parameters, that are functions of $\delta, \phi_{1,2}$ and the leptogenesis phases,
- Extract the effects of the known values of δ and $\phi_{1,2}$, and isolate the leptogenesis parameters.

In the absence of complete information on the first two steps above, we are currently at the stage of preliminary explorations of the multi-dimensional parameter space. As seen in Fig. 20, the amount of the leptogenesis asymmetry is explicitly independent of δ ⁵⁰. However, in order to make more definite predictions, one must make extra hypotheses.

One possibility is that the inflaton might be a heavy singlet sneutrino, as discussed in the previous Lecture¹⁰⁵. As shown there, this hypothesis would require a mass $\simeq 1.8 \times 10^{13}$ GeV for the lightest sneutrino, which is well within the range favoured by seesaw models. As also discussed in the previous Lecture, this sneutrino inflaton model predicts values of the spectral index of scalar perturbations, the fraction of tensor perturbations and other CMB observables that are consistent

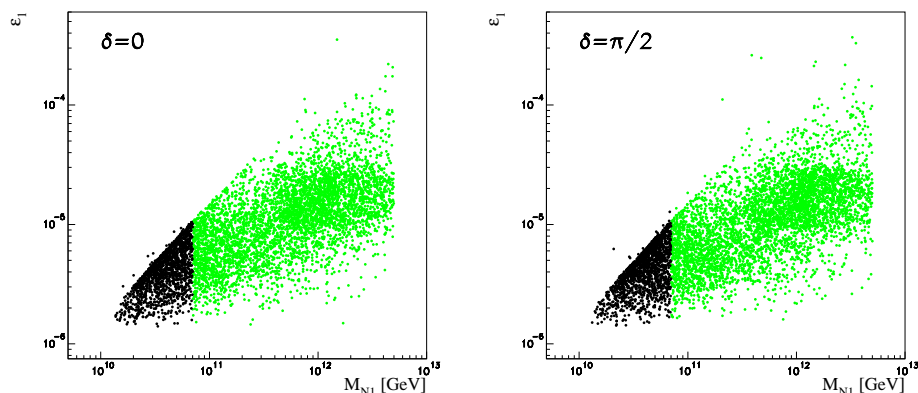


Figure 20. Comparison of the CP-violating asymmetries in the decays of heavy singlet neutrinos giving rise to the cosmological baryon asymmetry via leptogenesis (left panel) without and (right panel) with maximal CP violation in neutrino oscillations⁵⁰. They are indistinguishable.

with the WMAP data. The sneutrino inflaton model is quite compatible with a low reheating temperature, as seen in Fig. 19. Moreover, because of this and the other constraints on the seesaw model parameters in this model, it makes predictions for the branching ratio for $\mu \rightarrow e\gamma$ that are more precise than in the generic seesaw model. As seen in Fig. 21, it predicts that this decay should appear within a couple of orders of magnitude of the present experimental upper limit¹⁰⁵.

5.4 Ultra-High-Energy Cosmic Rays

The flux of cosmic rays falls approximately as E^{-3} from $E \sim 1$ GeV, through $E \sim 10^6$ GeV where there is a small change in slope called the ‘knee’, continuing to about 10^{10} GeV, the ‘ankle’. Beyond about 5×10^{10} GeV, as seen in Fig. 22, one expects a cutoff¹¹⁹ due to the photopion reaction $p + \gamma_{CMB} \rightarrow \Delta^+ \rightarrow p + \bar{\pi}^0, n + \pi^+$, for all primary cosmic rays that originate from more than about 50 Mpc away. However, some experiments report cosmic-ray events with higher energies of 10^{11} GeV or more¹⁰⁹. If this excess flux beyond the GKZ cutoff is confirmed, conventional physics would require it to originate from distances $\lesssim 100$ Mpc, in which case one would expect to see some discrete sources. Analogous cutoffs are expected for primary cosmic-ray photons or nuclei, as also seen in Fig. 22.

There are two general categories of sources considered for such ultra-high-energy cosmic rays (UHECRs): *bottom-up* and *top-down* scenarios¹⁰⁹.

Astrophysical sources capable of accelerating high-energy cosmic rays in some bottom-up scenario must be larger than the gyromagnetic radius R corresponding

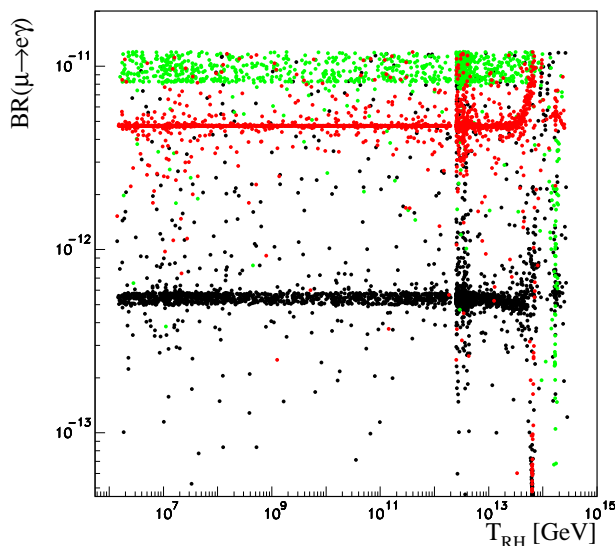


Figure 21. Calculations of $BR(\mu \rightarrow e\gamma)$ in the sneutrino inflation model. Black points correspond to $\sin \theta_{13} = 0.0$, $M_2 = 10^{14}$ GeV, and 5×10^{14} GeV $< M_3 < 5 \times 10^{15}$ GeV. Red points correspond to $\sin \theta_{13} = 0.0$, $M_2 = 5 \times 10^{14}$ GeV and $M_3 = 5 \times 10^{15}$ GeV, while green points correspond to $\sin \theta_{13} = 0.1$, $M_2 = 10^{14}$ GeV and $M_3 = 5 \times 10^{14}$ GeV¹⁰⁵. We assume for illustration that $(m_{1/2}, m_0) = (800, 170)$ GeV and $\tan \beta = 10$.

to their internal magnetic field B :

$$R \sim \left(\frac{100}{Z} \right) \left(\frac{E}{10^{11} \text{ GeV}} \right) \left(\frac{\mu G}{B} \right) \text{ kpc}, \quad (152)$$

where Z is the atomic number of the cosmic ray particle. Candidate astrophysical sources include gamma-ray busters (GRBs) and active galactic nuclei (AGNs).

If UHECRs are produced by such localized sources, one would expect to see a clustering in their arrival directions. Such clustering has been claimed in both the AGASA and Yakutsk data¹²⁰, but I personally do not find the evidence overwhelming. A correlation has also been claimed with BL Lac objects¹²¹, which are AGNs emitting relativistic jets pointing towards us, but this is also a claim that I should like to see confirmed by more data, as will be provided soon by the HiRes and Auger experiments.

Favoured top-down scenarios involve physics at the GUT scale $\gtrsim 10^{15}$ GeV that produces UHECRs with energies $\sim 10^{12}$ GeV via some ‘trickle-down’ mechanism. Suggestions have included topological structures, such as cosmic strings, that are present in some GUTs and would radiate energetic particles, and the decays of

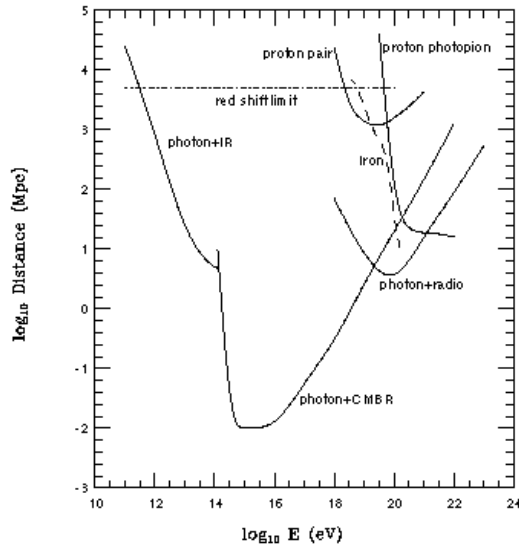


Figure 22. Energetic particles propagating through the Universe scatter on relic photons, imposing a cutoff on the maximum distance over which they can propagate ¹¹⁹.

metastable superheavy relic particles.

In the latter case, one would expect most of the observed UHECRs to come from the decays of relics in our own galactic halo. In this case, one would expect the UHECRs to exhibit an anisotropy correlated with the orientation of the galaxy ¹²². The present data are insufficient to confirm or exclude an isotropy of the magnitude predicted in different halo models, but the Auger experiment should be able to decide the issue. One might naively expect that superheavy relic particles would be spread smoothly through the halo, and hence that they would not cause clustering in the UHECRs. However, this is not necessarily the case, as many cold dark matter models predict clumps within the halo ¹²³, which could contribute a clustered component on top of an apparently smooth background.

How might suitable metastable superheavy relic particles arise ¹²⁴? The proton is a prototype for a metastable particle. As discussed earlier in this Lecture, we know that its lifetime must exceed about 10^{33} y or so, much longer than if it decayed via conventional weak interactions. On the other hand, there is no known exact symmetry principle capable of preventing the proton from decaying. Therefore, we believe that it is only metastable, decaying very slowly via some higher-dimensional non-renormalizable interaction that violates baryon number. For example, as we saw earlier, in many GUT models there is a dimension-6 $qqq\ell$ interaction with a coefficient $\propto 1/M^2$, where M is some superheavy mass scale. This would yield a decay amplitude $A \sim 1/M^2$, and hence a long lifetime $\tau \sim \frac{M^4}{m_p^5}$.

We must work harder in the case of a superheavy relic weighing $\gtrsim 10^{12}$ GeV,

but the principle is the same. For an interaction of dimension $4 + n$, we expect

$$\tau \sim \frac{M^{2n}}{m_{\text{relic}}^{2n+1}} \quad (153)$$

This could yield a lifetime greater than the age of the Universe, even for $m_{\text{relic}} \sim 10^{12}$ GeV, if M and/or n are large enough, for example if $M \sim 10^{17}$ GeV and $n \geq 9$ ¹²⁵.

Phenomenological constraints on such metastable relic particles were considered some time ago for reasons other than explaining UHECRs ¹²⁶. Constraints from the abundances of light elements, from the CMB and from the high-energy ν flux have been considered. They provide no obstacle to postulating a superheavy relic particle with $\Omega h^2 \sim 0.1$ if $\tau \gtrsim 10^{15}$ y. Hence, metastable superheavy relic particles could in principle constitute most of the cold dark matter.

Possible theoretical candidates within a general framework of string and/or M theory have been considered ^{124,125}. These models have the generic feature that, in addition to the interactions of the Standard Model, there are others that act on a different set of ‘hidden’ matter particles, which communicate with the Standard Model only via higher-order interactions scaled by some inverse power of a large mass scale M . Just as the strong nuclear interactions bind quarks to form metastable massive particles, the protons, so some ‘hidden-sector’ interactions might become strong at some higher energy scale, and form analogous, but supermassive, metastable particles. Just like the proton, these massive ‘cryptons’ generally decay through high-dimension interactions into multiple quarks and leptons. The energetic quarks hadronize via QCD in a way that can be modelled using information from Z^0 decays at LEP. Several simulations have shown that the resulting spectrum of UHECRs is compatible with the available data, whether supersymmetry is included in the jet fragmentation process, or not, as shown in Fig. 23 ¹²⁷.

A crucial issue is whether there is a mechanism that might produce a relic density of superheavy particles that is large enough to be of interest for cosmology, without being excessive. As was discussed in Lecture 3, the plausible upper limit on the mass of a relic particle that was initially in thermal equilibrium is of the order of a TeV. However, equilibrium might have been violated in the early Universe, around the epoch of inflation, and various non-thermal production mechanisms have been proposed ¹²⁸. These include out-of-equilibrium processes at the end of the inflationary epoch, such as parametric resonance effects, and gravitational production as the scale factor of the Universe changes rapidly. It is certainly possible that superheavy relic particles might be produced with a significant fraction of the critical density.

We have seen that UHECRs could perhaps be due to the decays of metastable superheavy relic particles. They might have the appropriate abundance, their lifetimes might be long on a cosmological time-scale, and the decay spectrum might be compatible with the events seen. Pressure points on this interpretation of UHECRs include the composition of the UHECRs – there should be photons and possibly neutrinos, as well as protons, and no heavier nuclei; their isotropy – UHECRs from relic decays would exhibit a detectable galactic anisotropy; and clustering – this

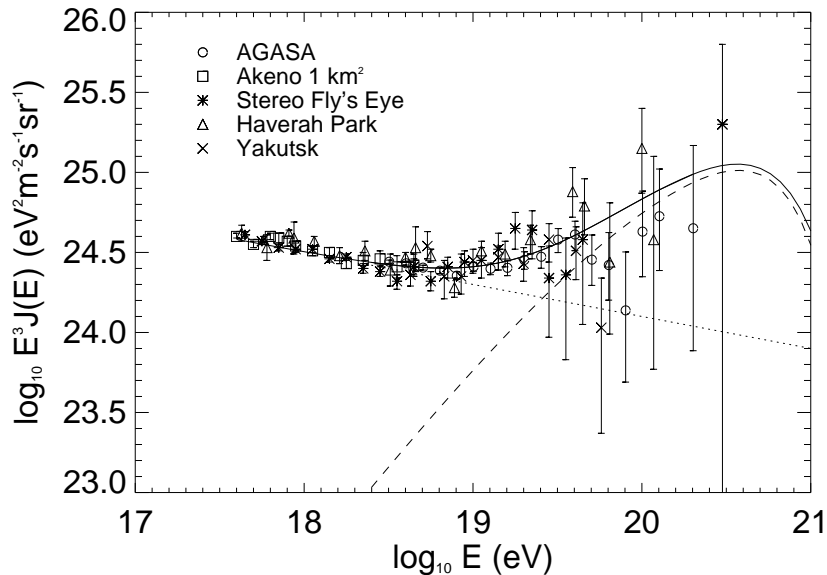


Figure 23. The spectrum of UHECRs can be explained by the decays of superheavy metastable particles such as cryptons ¹²⁷.

would certainly be expected in astrophysical source models, but is not excluded in the superheavy relic interpretation.

The Auger project currently under construction in Argentina should provide much greater statistics on UHECRs and be able to address many of these issues ¹²⁹. In the longer term, the EUSO project now being considered by ESA for installation on the International Space Station would provide even greater sensitivity to UHECRs ¹³⁰. Thus an experimental programme exists in outline that is capable of clarifying their nature and origin, telling us whether they are indeed due to new fundamental physics.

5.5 Summary

We have seen in these lectures that the Standard Model must underlie any description of the physics of the early Universe. Its extensions may provide the answers to many of the outstanding issues in cosmology, such as the nature of dark matter, the origin of the matter in the Universe, the size and age of the Universe, and the origins of the structures within it. Theories capable of resolving these issues abound, and include many new options not stressed in these lectures. Continued progress in understanding these issues will involve a complex interplay between particle physics and cosmology, involving experiments at new accelerators such as the LHC, as well as new observations.

References

1. C. Lineweaver, Lectures at this School.
2. For a recent review, see: K. A. Olive, arXiv:astro-ph/0202486.
3. E. W. Kolb and M. S. Turner, *The Early Universe* (Addison-Wesley, Redwood City, USA, 1990).
4. See the LHC home page:
<http://lhc-new-homepage.web.cern.ch/lhc-new-homepage/>.
5. S.L. Glashow, *Nucl. Phys.* **22**, 579 (1961); S. Weinberg, *Phys. Rev. Lett.* **19**, 1264 (1967); A. Salam, Proc. 8th Nobel Symposium, Stockholm 1968, ed. N. Svartholm (Almqvist and Wiksells, Stockholm, 1968), p. 367.
6. LEP Electroweak Working Group,
<http://lepewwg.web.cern.ch/LEPEWWG/Welcome.html>.
7. C. Bouchiat, J. Iliopoulos and Ph. Meyer, *Phys. Lett. B* **138**, 652 (1972) and references therein.
8. C. Quigg, *Gauge Theories of the Strong, Weak and Electromagnetic Interactions* (Benjamin-Cummings, Reading, 1983).
9. D. Brandt, H. Burkhardt, M. Lamont, S. Myers and J. Wenninger, *Rept. Prog. Phys.* **63**, 939 (2000).
10. M. Veltman, *Nucl. Phys. B* **123**, 89 (1977); M.S. Chanowitz, M. Furman and I. Hinchliffe, *Phys. Lett. B* **78**, 285 (1978).
11. M. Veltman, *Acta Phys.Pol.* **8**, 475 (1977).
12. J. R. Ellis, M. K. Gaillard and D. V. Nanopoulos, *Nucl. Phys. B* **106**, 292 (1976).
13. LEP Higgs Working Group for Higgs boson searches, OPAL Collaboration, ALEPH Collaboration, DELPHI Collaboration and L3 Collaboration, *Search for the Standard Model Higgs Boson at LEP*, CERN-EP/2003-011.
14. J. R. Ellis, Lectures at 1998 CERN Summer School, St. Andrews, *Beyond the Standard Model for Hillwalkers*, arXiv:hep-ph/9812235.
15. J. R. Ellis, Lectures at 2001 CERN Summer School, Beatenberg, *Supersymmetry for Alp hikers*, arXiv:hep-ph/0203114.
16. J. Scherk and J. H. Schwarz, *Nucl. Phys.* **B81**, 118 (1974); M. B. Green and J. H. Schwarz, *Phys. Lett.* **149B**, 117 (1984) and **151B**, 21 (1985); J. R. Ellis, *The Superstring: Theory Of Everything, Or Of Nothing?*, *Nature* **323**, 595 (1986).
17. K. Hagiwara *et al.* [Particle Data Group Collaboration], *Phys. Rev. D* **66**, 010001 (2002).
18. A. Osipowicz *et al.* [KATRIN Collaboration], arXiv:hep-ex/0109033.
19. O. Elgaroy *et al.*, *Phys. Rev. Lett.* **89**, 061301 (2002) [arXiv:astro-ph/0204152].
20. C. L. Bennett *et al.*, arXiv:astro-ph/0302207; D. N. Spergel *et al.*, arXiv:astro-ph/0302209; H. V. Peiris *et al.*, arXiv:astro-ph/0302225.
21. H. V. Klapdor-Kleingrothaus *et al.*, *Eur. Phys. J. A* **12**, 147 (2001) [arXiv:hep-ph/0103062]; see, however, H. V. Klapdor-Kleingrothaus *et al.*, *Mod. Phys. Lett. A* **16**, 2409 (2002) [arXiv:hep-ph/0201231].
22. Y. Fukuda *et al.* [Super-Kamiokande Collaboration], *Phys. Rev. Lett.* **81**,

- 1562 (1998) [arXiv:hep-ex/9807003].
23. Q. R. Ahmad *et al.* [SNO Collaboration], *Phys. Rev. Lett.* **89**, 011301 (2002) [arXiv:nucl-ex/0204008]; *Phys. Rev. Lett.* **89**, 011302 (2002) [arXiv:nucl-ex/0204009].
 24. R. Barbieri, J. R. Ellis and M. K. Gaillard, *Phys. Lett. B* **90**, 249 (1980).
 25. M. Gell-Mann, P. Ramond and R. Slansky, Proceedings of the Supergravity Stony Brook Workshop, New York, 1979, eds. P. Van Nieuwenhuizen and D. Freedman (North-Holland, Amsterdam); T. Yanagida, Proceedings of the Workshop on Unified Theories and Baryon Number in the Universe, Tsukuba, Japan 1979 (edited by A. Sawada and A. Sugamoto, KEK Report No. 79-18, Tsukuba); R. Mohapatra and G. Senjanovic, *Phys. Rev. Lett.* **44**, 912 (1980).
 26. P. H. Frampton, S. L. Glashow and T. Yanagida, arXiv:hep-ph/0208157.
 27. T. Endoh, S. Kaneko, S. K. Kang, T. Morozumi and M. Tanimoto, arXiv:hep-ph/0209020.
 28. J. R. Ellis, J. S. Hagelin, S. Kelley and D. V. Nanopoulos, *Nucl. Phys. B* **311**, 1 (1988).
 29. J. R. Ellis, M. E. Gómez, G. K. Leontaris, S. Lola and D. V. Nanopoulos, *Eur. Phys. J. C* **14**, 319 (2000).
 30. J. R. Ellis, M. K. Gaillard and D. V. Nanopoulos, *Nucl. Phys. B* **109**, 213 (1976).
 31. M. Kobayashi and T. Maskawa, *Prog. Theor. Phys.* **49**, 652 (1973).
 32. Z. Maki, M. Nakagawa and S. Sakata, *Prog. Theor. Phys.* **28**, 870 (1962).
 33. Y. Oyama, arXiv:hep-ex/0210030.
 34. S. Fukuda *et al.* [Super-Kamiokande Collaboration], *Phys. Lett. B* **539**, 179 (2002) [arXiv:hep-ex/0205075].
 35. S. A. Dazeley [KamLAND Collaboration], arXiv:hep-ex/0205041.
 36. S. Pakvasa and J. W. Valle, arXiv:hep-ph/0301061.
 37. H. Minakata and H. Sugiyama, arXiv:hep-ph/0212240.
 38. Chooz Collaboration, *Phys. Lett. B* **420**, 397 (1998).
 39. A. De Rújula, M.B. Gavela and P. Hernández, *Nucl. Phys. B* **547**, 21 (1999) [arXiv:hep-ph/9811390].
 40. A. Cervera *et al.*, *Nucl. Phys. B* **579**, 17 (2000) [Erratum-ibid. *B* **593**, 731 (2001)].
 41. B. Autin *et al.*, *Conceptual design of the SPL, a high-power superconducting H^- linac at CERN*, CERN-2000-012.
 42. P. Zucchelli, *Phys. Lett. B* **532**, 166 (2002).
 43. M. Apollonio *et al.*, *Oscillation physics with a neutrino factory*, arXiv:hep-ph/0210192; and references therein.
 44. J. A. Casas and A. Ibarra, *Nucl. Phys. B* **618**, 171 (2001) [arXiv:hep-ph/0103065].
 45. J. R. Ellis, J. Hisano, S. Lola and M. Raidal, *Nucl. Phys. B* **621**, 208 (2002) [arXiv:hep-ph/0109125].
 46. S. Davidson and A. Ibarra, *JHEP* **0109**, 013 (2001).
 47. J. R. Ellis, J. Hisano, M. Raidal and Y. Shimizu, *Phys. Lett. B* **528**, 86 (2002) [arXiv:hep-ph/0111324].
 48. J. R. Ellis, J. Hisano, M. Raidal and Y. Shimizu, *Phys. Rev. D* **66**, 115013

- (2002) [arXiv:hep-ph/0206110].
49. M. Fukugita and T. Yanagida, *Phys. Lett. B* **174**, 45 (1986).
 50. J. R. Ellis and M. Raidal, *Nucl. Phys. B* **643**, 229 (2002) [arXiv:hep-ph/0206174].
 51. L. Maiani, *Proceedings of the 1979 Gif-sur-Yvette Summer School On Particle Physics*, 1; G. 't Hooft, in *Recent Developments in Gauge Theories, Proceedings of the Nato Advanced Study Institute, Cargese, 1979*, eds. G. 't Hooft *et al.*, (Plenum Press, NY, 1980); E. Witten, *Phys. Lett. B* **105**, 267 (1981).
 52. S. Ferrara, J. Wess and B. Zumino, *Phys. Lett. B* **51**, 239 (1974); S. Ferrara, J. Iliopoulos and B. Zumino, *Nucl. Phys. B* **77**, 413 (1974).
 53. P. Fayet, as reviewed in *Supersymmetry, Particle Physics And Gravitation*, CERN-TH-2864, published in *Proc. of Europhysics Study Conf. on Unification of Fundamental Interactions*, Erice, Italy, Mar 17-24, 1980, eds. S. Ferrara, J. Ellis, P. van Nieuwenhuizen (Plenum Press, 1980).
 54. R. Haag, J. Lopuszanski and M. Sohnius, *Nucl. Phys. B* **88**, 257 (1975).
 55. H. E. Haber and G. L. Kane, *Phys. Rep.* **117**, 75 (1985).
 56. J. Ellis, S. Kelley and D. V. Nanopoulos, *Phys. Lett. B* **260**, 131 (1991); U. Amaldi, W. de Boer and H. Furstenu, *Phys. Lett. B* **260**, 447 (1991); P. Langacker and M. x. Luo, *Phys. Rev. D* **44**, 817 (1991); C. Giunti, C. W. Kim and U. W. Lee, *Mod. Phys. Lett. A* **6**, 1745 (1991).
 57. H. Georgi, H. R. Quinn and S. Weinberg, *Phys. Rev. Lett.* **33**, 451 (1974).
 58. Y. Okada, M. Yamaguchi and T. Yanagida, *Prog. Theor. Phys.* **85**, 1 (1991); J. R. Ellis, G. Ridolfi and F. Zwirner, *Phys. Lett. B* **257**, 83 (1991); H. E. Haber and R. Hempfling, *Phys. Rev. Lett.* **66**, 1815 (1991).
 59. J. Ellis, J. S. Hagelin, D. V. Nanopoulos, K. A. Olive and M. Srednicki, *Nucl. Phys. B* **238**, 453 (1984).
 60. H. Goldberg, *Phys. Rev. Lett.* **50**, 1419 (1983).
 61. G. W. Bennett *et al.* [Muon g-2 Collaboration], *Phys. Rev. Lett.* **89**, 101804 (2002) [Erratum-ibid. **89**, 1219903 (2002)] [arXiv:hep-ex/0208001].
 62. M. Davier, S. Eidelman, A. Hocker and Z. Zhang, arXiv:hep-ph/0208177; see also K. Hagiwara, A. D. Martin, D. Nomura and T. Teubner, arXiv:hep-ph/0209187; F. Jegerlehner, unpublished, as reported in M. Krawczyk, arXiv:hep-ph/0208076.
 63. Joint LEP 2 Supersymmetry Working Group, *Combined LEP Chargino Results, up to 208 GeV*, http://lepsusy.web.cern.ch/lepsusy/www/inos_moriond01/charginos_pub.html.
 64. Joint LEP 2 Supersymmetry Working Group, *Combined LEP Selection/Smuon/Stau Results, 183-208 GeV*, http://lepsusy.web.cern.ch/lepsusy/www/sleptons_summer02/slep_2002.html.
 65. J. Ellis, K. A. Olive, Y. Santoso and V. C. Spanos, arXiv:hep-ph/0303043.
 66. M. S. Alam *et al.*, [CLEO Collaboration], *Phys. Rev. Lett.* **74**, 2885 (1995), as updated in S. Ahmed *et al.*, CLEO CONF 99-10; BELLE Collaboration, BELLE-CONF-0003, contribution to the 30th International conference on High-Energy Physics, Osaka, 2000. See also K. Abe *et al.*,

- [Belle Collaboration], arXiv:hep-ex/0107065; L. Lista [BaBar Collaboration], arXiv:hep-ex/0110010; C. Degrandi, P. Gambino and G. F. Giudice, *JHEP* **0012**, 009 (2000) [arXiv:hep-ph/0009337]; M. Carena, D. Garcia, U. Nierste and C. E. Wagner, *Phys. Lett. B* **499**, 141 (2001) [arXiv:hep-ph/0010003].
67. J. R. Ellis, G. Gani, D. V. Nanopoulos and K. A. Olive, *Phys. Lett. B* **502**, 171 (2001) [arXiv:hep-ph/0009355].
 68. H. N. Brown *et al.* [Muon g-2 Collaboration], *Phys. Rev. Lett.* **86**, 2227 (2001) [arXiv:hep-ex/0102017].
 69. M. Knecht and A. Nyffeler, arXiv:hep-ph/0111058; M. Knecht, A. Nyffeler, M. Perrottet and E. De Rafael, arXiv:hep-ph/0111059; M. Hayakawa and T. Kinoshita, arXiv:hep-ph/0112102; I. Blokland, A. Czarnecki and K. Melnikov, arXiv:hep-ph/0112117; J. Bijnens, E. Pallante and J. Prades, arXiv:hep-ph/0112255.
 70. L. L. Everett, G. L. Kane, S. Rigolin and L. Wang, *Phys. Rev. Lett.* **86**, 3484 (2001) [arXiv:hep-ph/0102145]; J. L. Feng and K. T. Matchev, *Phys. Rev. Lett.* **86**, 3480 (2001) [arXiv:hep-ph/0102146]; E. A. Baltz and P. Gondolo, *Phys. Rev. Lett.* **86**, 5004 (2001) [arXiv:hep-ph/0102147]; U. Chattopadhyay and P. Nath, *Phys. Rev. Lett.* **86**, 5854 (2001) [arXiv:hep-ph/0102157]; S. Komine, T. Moroi and M. Yamaguchi, *Phys. Lett. B* **506**, 93 (2001) [arXiv:hep-ph/0102204]; J. Ellis, D. V. Nanopoulos and K. A. Olive, *Phys. Lett. B* **508**, 65 (2001) [arXiv:hep-ph/0102331]; R. Arnowitt, B. Dutta, B. Hu and Y. Santoso, *Phys. Lett. B* **505**, 177 (2001) [arXiv:hep-ph/0102344]; S. P. Martin and J. D. Wells, *Phys. Rev. D* **64**, 035003 (2001) [arXiv:hep-ph/0103067]; H. Baer, C. Balazs, J. Ferrandis and X. Tata, *Phys. Rev. D* **64**, 035004 (2001) [arXiv:hep-ph/0103280].
 71. S. Mizuta and M. Yamaguchi, *Phys. Lett. B* **298**, 120 (1993) [arXiv:hep-ph/9208251]; J. Edsjo and P. Gondolo, *Phys. Rev. D* **56**, 1879 (1997) [arXiv:hep-ph/9704361].
 72. J. Ellis, T. Falk and K. A. Olive, *Phys. Lett. B* **444**, 367 (1998) [arXiv:hep-ph/9810360]; J. Ellis, T. Falk, K. A. Olive and M. Srednicki, *Astropart. Phys.* **13**, 181 (2000) [arXiv:hep-ph/9905481]; M. E. Gómez, G. Lazarides and C. Pallis, *Phys. Rev. D* **61**, 123512 (2000) [arXiv:hep-ph/9907261] and *Phys. Lett. B* **487**, 313 (2000) [arXiv:hep-ph/0004028]; R. Arnowitt, B. Dutta and Y. Santoso, *Nucl. Phys. B* **606**, 59 (2001) [arXiv:hep-ph/0102181].
 73. M. Drees and M. M. Nojiri, *Phys. Rev. D* **47**, 376 (1993) [arXiv:hep-ph/9207234]; H. Baer and M. Brhlik, *Phys. Rev. D* **53**, 597 (1996) [arXiv:hep-ph/9508321] and *Phys. Rev. D* **57**, 567 (1998) [arXiv:hep-ph/9706509]; H. Baer, M. Brhlik, M. A. Diaz, J. Ferrandis, P. Mercadante, P. Quintana and X. Tata, *Phys. Rev. D* **63**, 015007 (2001) [arXiv:hep-ph/0005027]; A. B. Lahanas, D. V. Nanopoulos and V. C. Spanos, *Mod. Phys. Lett. A* **16**, 1229 (2001) [arXiv:hep-ph/0009065].
 74. J. R. Ellis, T. Falk, G. Gani, K. A. Olive and M. Srednicki, *Phys. Lett. B* **510**, 236 (2001) [arXiv:hep-ph/0102098].
 75. J. L. Feng, K. T. Matchev and T. Moroi, *Phys. Rev. Lett.* **84**, 2322 (2000) [arXiv:hep-ph/9908309]; J. L. Feng, K. T. Matchev and T. Moroi, *Phys. Rev.*

- D **61**, 075005 (2000) [arXiv:hep-ph/9909334]; J. L. Feng, K. T. Matchev and F. Wilczek, *Phys. Lett. B* **482**, 388 (2000) [arXiv:hep-ph/0004043].
76. M. Battaglia *et al.*, *Eur. Phys. J. C* **22**, 535 (2001) [arXiv:hep-ph/0106204].
77. J. R. Ellis and K. A. Olive, *Phys. Lett. B* **514**, 114 (2001) [arXiv:hep-ph/0105004].
78. J. Ellis, K. Enqvist, D. V. Nanopoulos and F. Zwirner, *Mod. Phys. Lett. A* **1**, 57 (1986); R. Barbieri and G. F. Giudice, *Nucl. Phys. B* **306**, 63 (1988).
79. G. L. Kane, J. Lykken, S. Mrenna, B. D. Nelson, L. T. Wang and T. T. Wang, arXiv:hep-ph/0209061.
80. D. R. Tovey, *Phys. Lett. B* **498**, 1 (2001) [arXiv:hep-ph/0006276].
81. F. E. Paige, hep-ph/0211017.
82. ATLAS Collaboration, *ATLAS detector and physics performance Technical Design Report*, CERN/LHCC 99-14/15 (1999); S. Abdullin *et al.* [CMS Collaboration], arXiv:hep-ph/9806366; S. Abdullin and F. Charles, *Nucl. Phys. B* **547**, 60 (1999) [arXiv:hep-ph/9811402]; CMS Collaboration, Technical Proposal, CERN/LHCC 94-38 (1994).
83. I. Hinchliffe, F. E. Paige, M. D. Shapiro, J. Soderqvist and W. Yao, *Phys. Rev. D* **55**, 5520 (1997).
84. J. R. Ellis, G. Ganiis and K. A. Olive, *Phys. Lett. B* **474**, 314 (2000) [arXiv:hep-ph/9912324].
85. J. Silk and M. Srednicki, *Phys. Rev. Lett.* **53**, 624 (1984).
86. J. Ellis, J. L. Feng, A. Ferstl, K. T. Matchev and K. A. Olive, arXiv:astro-ph/0110225.
87. J. Silk, K. A. Olive and M. Srednicki, *Phys. Rev. Lett.* **55**, 257 (1985).
88. M. W. Goodman and E. Witten, *Phys. Rev. D* **31**, 3059 (1985).
89. R. Bernabei *et al.* [DAMA Collaboration], *Phys. Lett. B* **436**, 379 (1998).
90. D. Abrams *et al.* [CDMS Collaboration], arXiv:astro-ph/0203500; A. Benoit *et al.* [EDELWEISS Collaboration], *Phys. Lett. B* **513**, 15 (2001) [arXiv:astro-ph/0106094].
91. R. W. Schnee *et al.* [CDMS Collaboration], *Phys. Rept.* **307**, 283 (1998).
92. M. Bravin *et al.* [CRESST Collaboration], *Astropart. Phys.* **12**, 107 (1999) [arXiv:hep-ex/9904005].
93. H. V. Klapdor-Kleingrothaus, arXiv:hep-ph/0104028.
94. G. Jungman, M. Kamionkowski and K. Griest, *Phys. Rept.* **267**, 195 (1996) [arXiv:hep-ph/9506380]; <http://t8web.lanl.gov/people/jungman/neut-package.html>.
95. D. H. Lyth and A. Riotto, *Phys. Rept.* **314**, 1 (1999) [arXiv:hep-ph/9807278].
96. A. H. Guth, *Phys. Rev. D* **23**, 347 (1981).
97. A. G. Riess *et al.* [Supernova Search Team Collaboration], *Astron. J.* **116**, 1009 (1998) [arXiv:astro-ph/9805201]; S. Perlmutter *et al.* [Supernova Cosmology Project Collaboration], *Astrophys. J.* **517**, 565 (1999) [arXiv:astro-ph/9812133]; Perlmutter, S. & Schmidt, B. P. 2003 arXiv:astro-ph/0303428; J. L. Tonry *et al.*, arXiv:astro-ph/0305008.
98. N. A. Bahcall, J. P. Ostriker, S. Perlmutter and P. J. Steinhardt, *Science* **284**, 1481 (1999) [arXiv:astro-ph/9906463].
99. A. D. Linde, *Phys. Lett. B* **108**, 389 (1982).

100. A. D. Linde, *Phys. Lett. B* **129**, 177 (1983).
101. D. La and P. J. Steinhardt, *Phys. Rev. Lett.* **62**, 376 (1989) [Erratum-ibid. **62**, 1066 (1989)].
102. J. R. Ellis, D. V. Nanopoulos, K. A. Olive and K. Tamvakis, *Phys. Lett. B* **118**, 335 (1982) and *Nucl. Phys. B* **221**, 524 (1983).
103. J. M. Bardeen, P. J. Steinhardt and M. S. Turner, *Phys. Rev. D* **28**, 679 (1983).
104. W. H. Kinney, arXiv:astro-ph/0301448.
105. J. R. Ellis, M. Raidal and T. Yanagida, arXiv:hep-ph/0303242.
106. V. Barger, H. S. Lee and D. Marfatia, arXiv:hep-ph/0302150.
107. H. Murayama, H. Suzuki, T. Yanagida and J. Yokoyama, *Phys. Rev. Lett.* **70**, 1912 (1993); H. Murayama, H. Suzuki, T. Yanagida and J. Yokoyama, *Phys. Rev. D* **50**, 2356 (1994) [arXiv:hep-ph/9311326].
108. A. D. Sakharov, *Pisma Zh. Eksp. Teor. Fiz.* **5**, 32 (1967)
109. M. Takeda *et al.*, arXiv:astro-ph/0209422; T. Abu-Zayyad *et al.* [High Resolution Fly's Eye Collaboration], arXiv:astro-ph/0208243 and arXiv:astro-ph/0208301.
110. H. Georgi and S.L. Glashow, *Phys. Rev. Lett.* **32**, 438 (1974).
111. S. Dimopoulos and H. Georgi, *Nucl. Phys. B* **193**, 50 (1981); S. Dimopoulos, S. Raby and F. Wilczek, *Phys. Rev. D* **24**, 1681 (1981); L. Ibàñez and G. G. Ross, *Phys. Lett. B* **105**, 439 (1981).
112. J. Ellis, M. K. Gaillard and D. V. Nanopoulos, *Phys. Lett. B* **91**, 67 (1980).
113. A. J. Buras, J. Ellis, M. K. Gaillard and D. V. Nanopoulos, *Nucl. Phys. B* **135**, 66 (1978).
114. M. Shiozawa *et al.* [Super-Kamiokande collaboration], *Phys. Rev. Lett.* **81**, 3319 (1998).
115. J. Ellis, D. V. Nanopoulos and S. Rudaz, *Nucl. Phys. B* **202**, 43 (1982); S. Dimopoulos, S. Raby and F. Wilczek, *Phys. Lett. B* **112**, 133 (1982).
116. S. Weinberg, *Phys. Rev. D* **26**, 287 (1982); N. Sakai and T. Yanagida, *Nucl. Phys. B* **197**, 533 (1982).
117. M. Yoshimura, *Phys. Rev. Lett.* **41**, 281 (1978) [Erratum-ibid. **42**, 746 (1979)].
118. J. R. Ellis, M. K. Gaillard and D. V. Nanopoulos, *Phys. Lett. B* **80**, 360 (1979) [Erratum-ibid. **82**, 464 (1979)].
119. K. Greisen, *Phys. Rev. Lett.* **16**, 748 (1966); G. T. Zatsepin and V. A. Kuzmin, *Pisma Zh. Eksp. Teor. Fiz.* **4**, 114 (1966).
120. P. G. Tinyakov and I. I. Tkachev, *Pisma Zh. Eksp. Teor. Fiz.* **74**, 3 (2001) [arXiv:astro-ph/0102101].
121. P. G. Tinyakov and I. I. Tkachev, *Pisma Zh. Eksp. Teor. Fiz.* **74**, 499 (2001) [arXiv:astro-ph/0102476] and arXiv:astro-ph/0301336. See, however, W. Evans, F. Ferrer and S. Sarkar, arXiv:astro-ph/0212533.
122. N. W. Evans, F. Ferrer and S. Sarkar, *Astropart. Phys.* **17**, 319 (2002) [arXiv:astro-ph/0103085].
123. M. G. Abadi, J. F. Navarro, M. Steinmetz and V. R. Eke, arXiv:astro-ph/0211331 and arXiv:astro-ph/0212282.
124. J. R. Ellis, J. L. Lopez and D. V. Nanopoulos, *Phys. Lett. B* **247**, 257

- (1990); V. Berezhinsky, M. Kachelriess and A. Vilenkin, *Phys. Rev. Lett.* **79**, 4302 (1997) [arXiv:astro-ph/9708217].
125. K. Benakli, J. R. Ellis and D. V. Nanopoulos, *Phys. Rev. D* **59**, 047301 (1999) [arXiv:hep-ph/9803333].
126. J. R. Ellis, G. B. Gelmini, J. L. Lopez, D. V. Nanopoulos and S. Sarkar, *Nucl. Phys. B* **373**, 399 (1992).
127. See, for example, M. Birkel and S. Sarkar, *Astropart. Phys.* **9**, 297 (1998) [arXiv:hep-ph/9804285].
128. See, for example, D. J. Chung, P. Crotty, E. W. Kolb and A. Riotto, *Phys. Rev. D* **64**, 043503 (2001) [arXiv:hep-ph/0104100].
129. A. Letessier-Selvon, arXiv:astro-ph/0208526; J. Cronin *et al.*, <http://www.auger.org/>.
130. L. Scarsi, *EUSO: Using high energy cosmic rays and neutrinos as messengers from the unknown universe*, in *Metepec 2000, Observing ultrahigh energy cosmic rays from space and earth*, p113.